NCMI

National Center for Macromolecular Imaging

Wah Chiu

wah@bcm.tmc.edu

Baylor College of Medicine

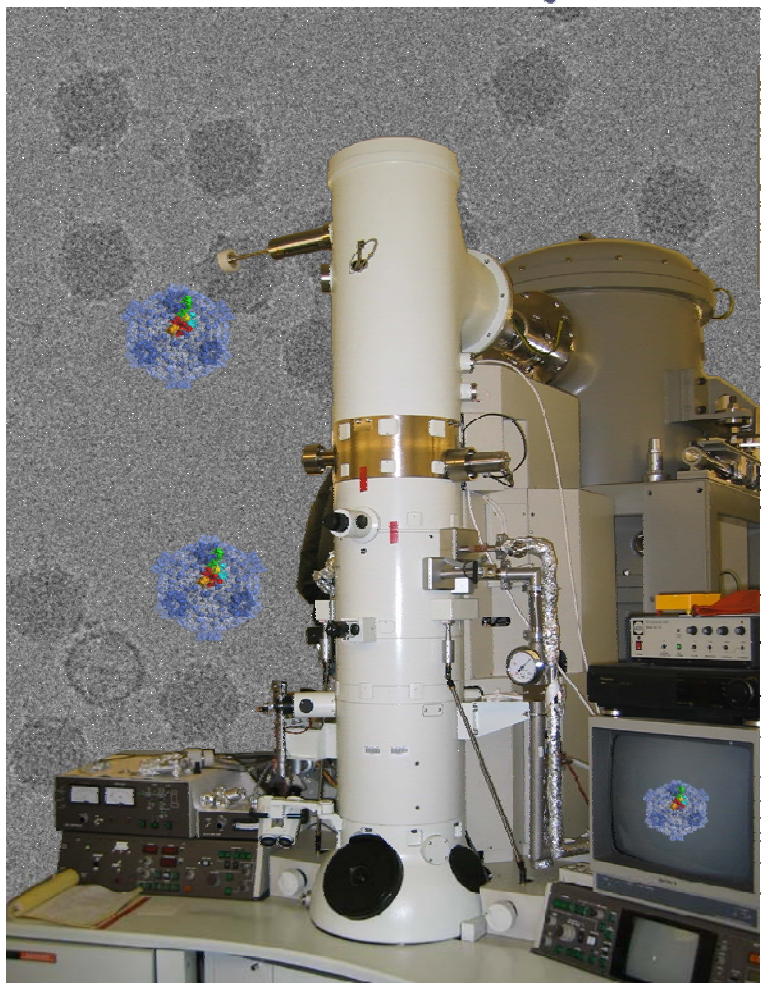

National Center for Research Resources

NSF

NIGMS

Trends in Macromolecular Cryo-EM

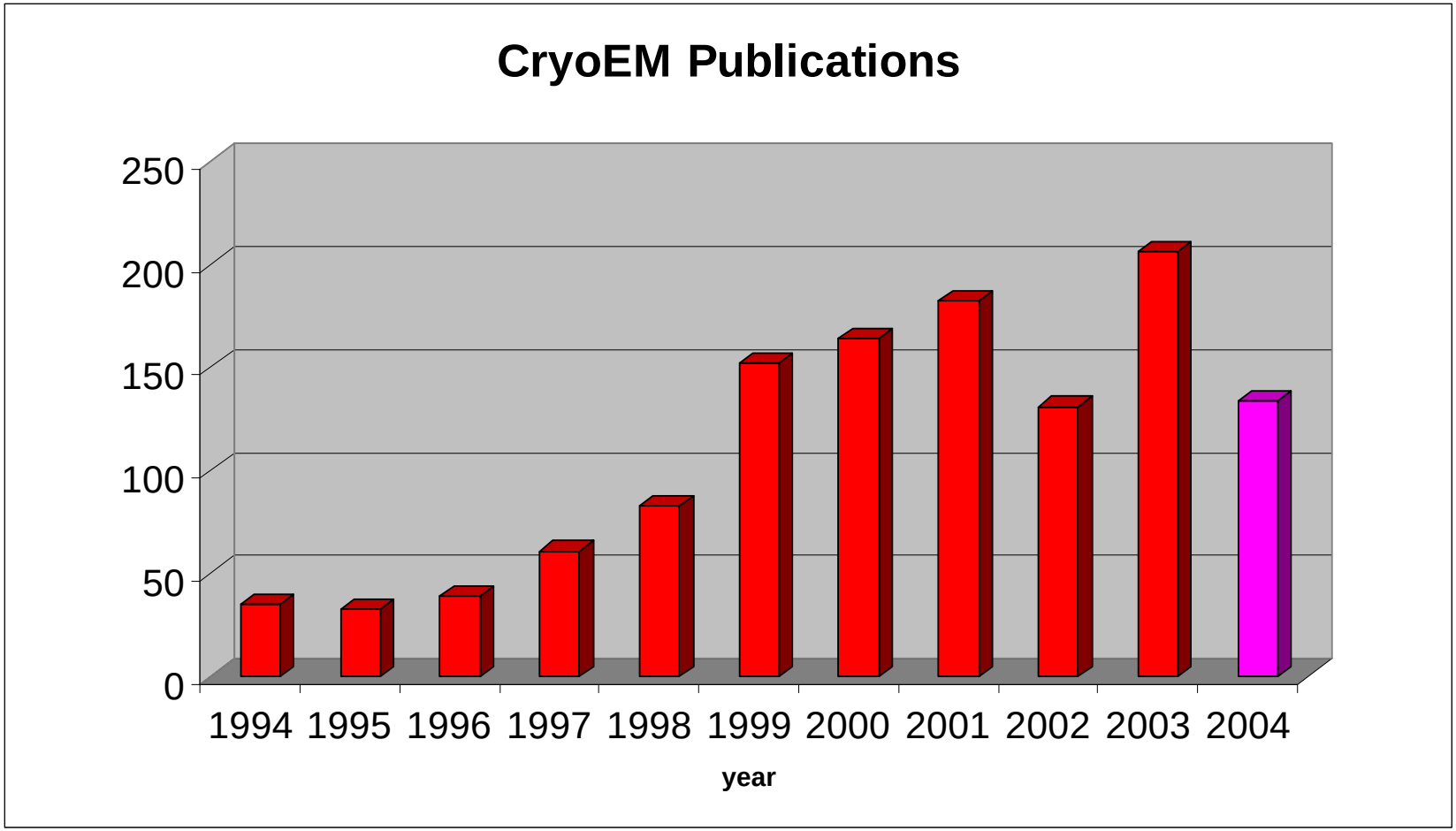

Surveyed in mid 2004

From Sample to Structure

biochemical preparation

cryo-em sample preparation

imaging

data collection

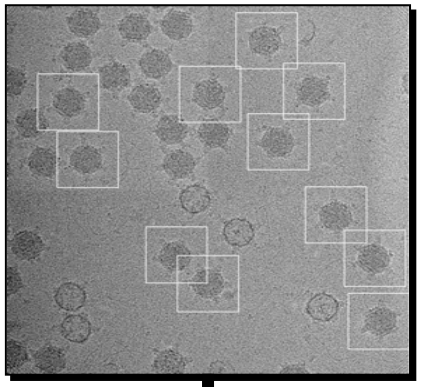

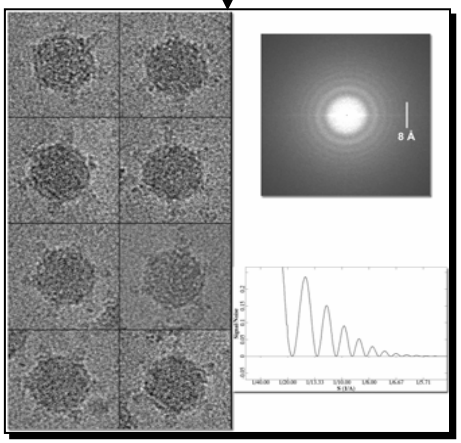

image processing

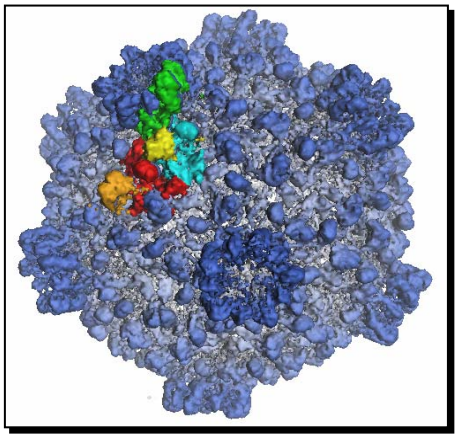

reconstruction

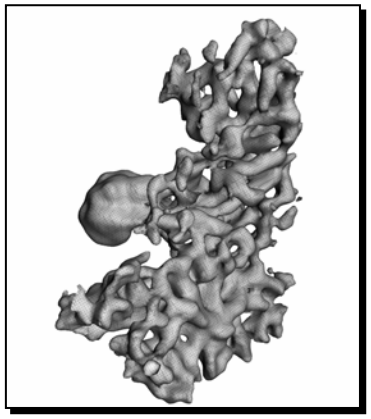

structural analysis

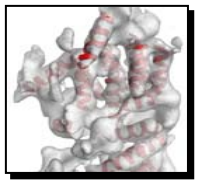

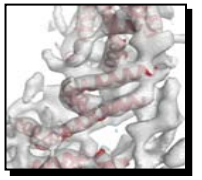

annotation

Image Contrast Theory

- Object is not too thick

  The allowable thickness is resolution dependent
- Image is a true 2-D projection of the 3-D object with the same focus throughout
- There is only elastically scattered electron in forming the image

Depth of Field Dependence on Resolution and Sample Thickness

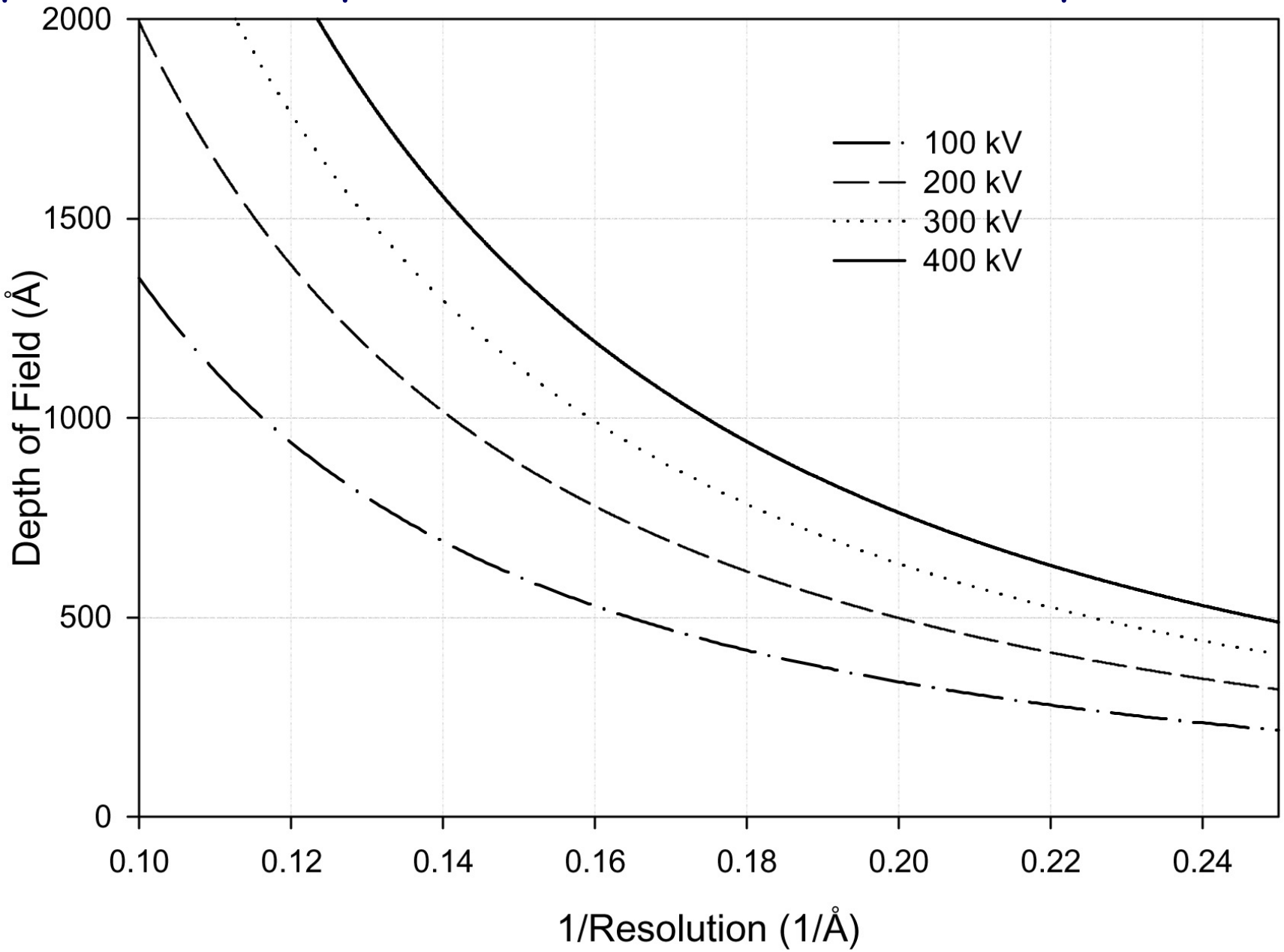

Zhou and Chiu, Adv Prot Chem 2003

3D Object

Projection Image

Fourier Transform

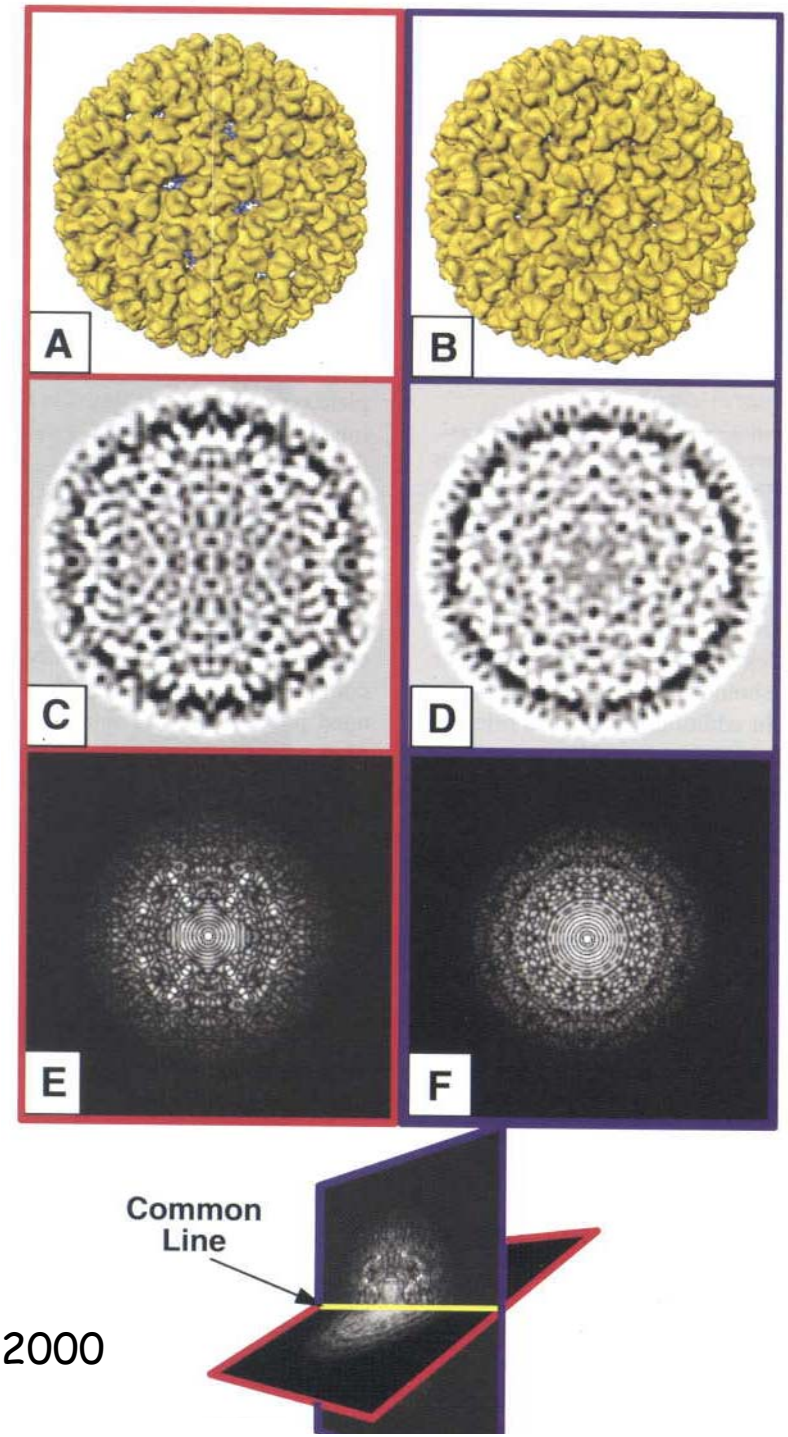

Thuman-Commike & Chiu, Micron 2000

Single Particle Images

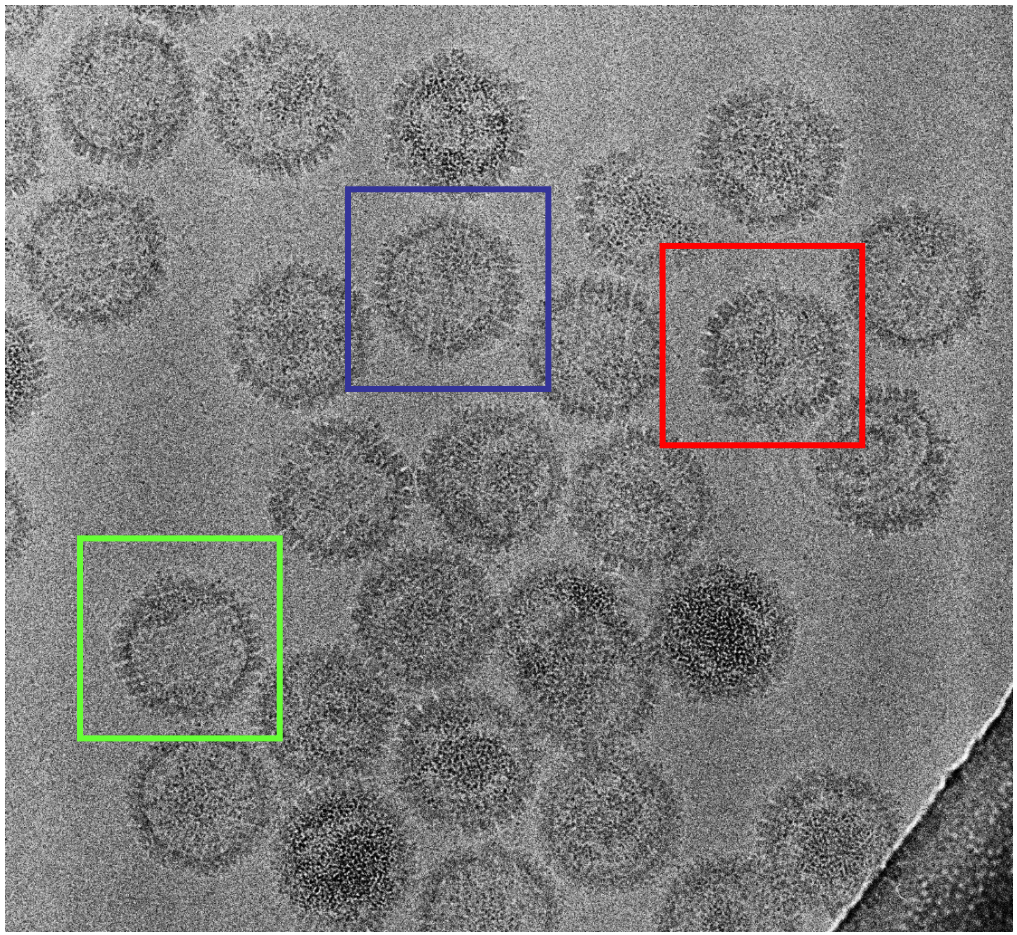

Equivalent data in Fourier space

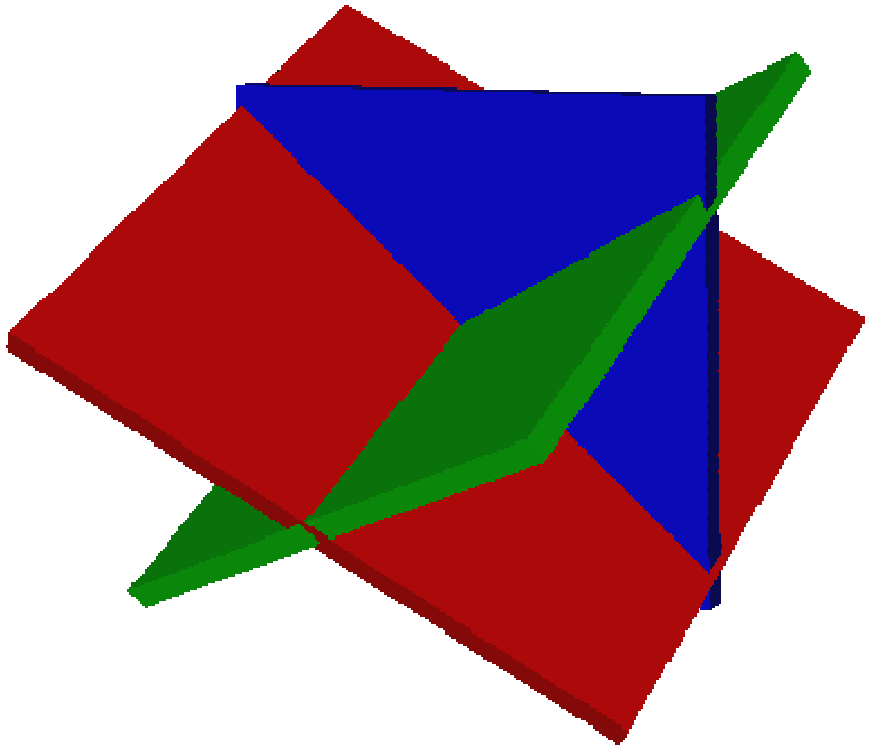

Hong Zhou

Concept of Fourier Analysis & Synthesis

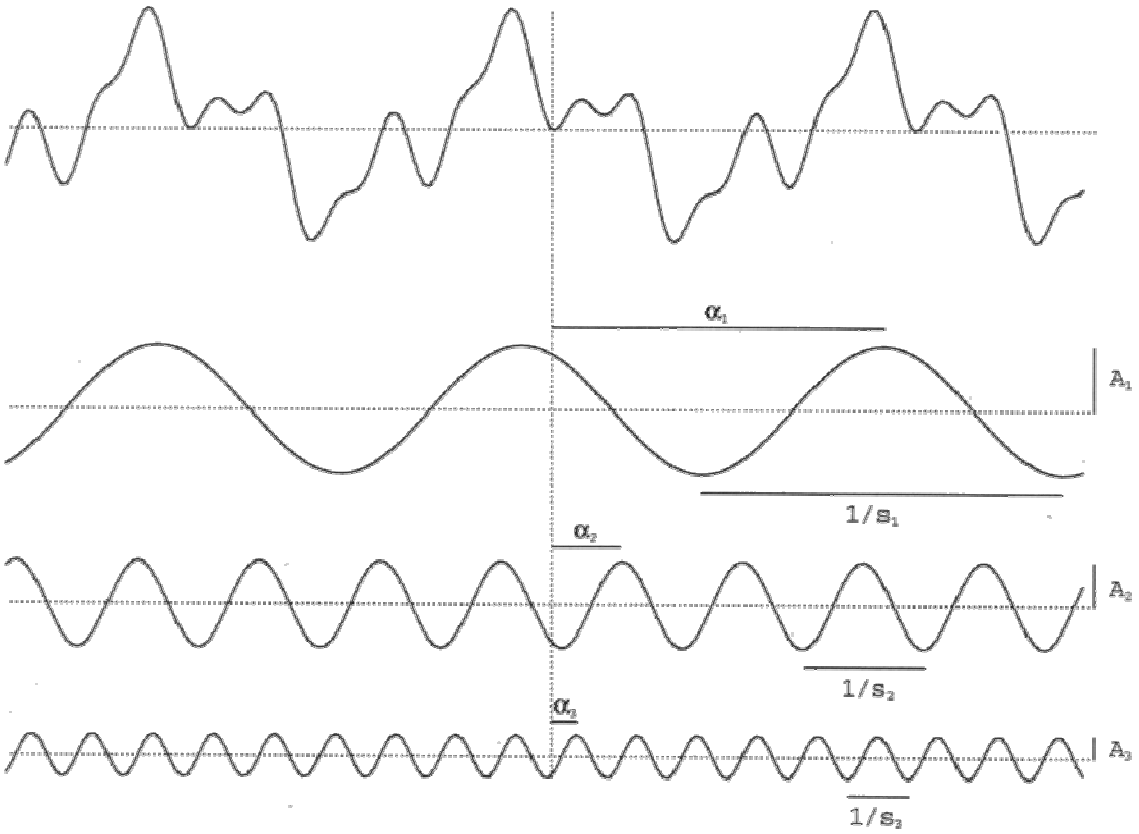

FIGURE 1 An illustration of a one-dimensional object potential function v(x) at the top of the figure which can be decomposed into three cosine waves with different frequencies (s), amplitudes (A), and phases (α) with respect to a common origin. The mathematical expression is $v(x) = \sum A_i(s) \cos(2\pi S_i x + \alpha_i)$. (provided by A. Avila-Sakar and V. Mootha)

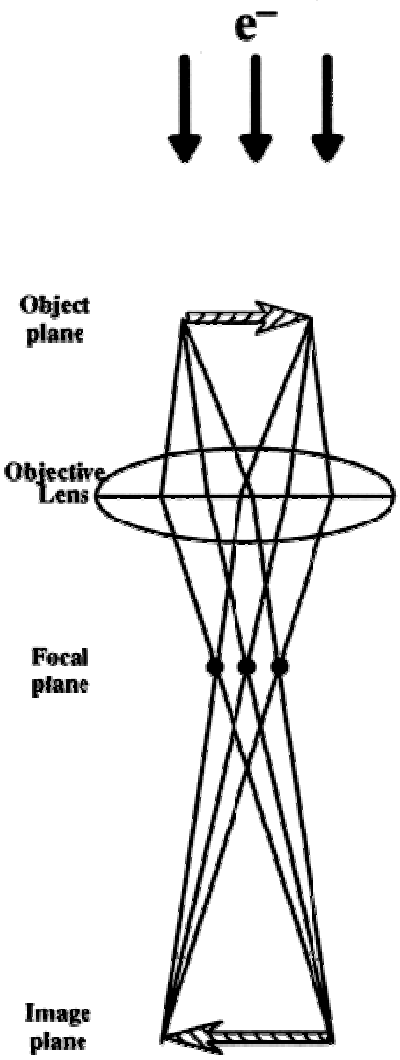

Object Coulomb potential function $V(x_o, y_o, z_o)$

Object transmitted wave function $\Psi_o(x_o, y_o)$

$$\Psi_o(x_o, y_o) \simeq 1 + i\sigma v(x_o, y_o)$$

$$v(x_o, y_o) = \int V(x_o, y_o, z_o)\, dz_o$$

Phase shift $\gamma(S)$ *introduced by objective lens*

$$\gamma(S) = 2\pi\left(\tfrac{1}{4} C_s \lambda^3 S^4 - \tfrac{1}{2} \Delta Z \lambda S^2\right)$$

Diffraction wave function $\Psi_d(S_x, S_y)$

$$\Psi_d(S_x, S_y) = F(S_x, S_y)\ exp\ (i\gamma(S))$$

$$F(S_x, S_y) = \mathcal{F}\,[\Psi_o(x_o, y_o)]$$

Diffraction intensity $I_d(S_x, S_y) = \Psi_d(S_x, S_y)\ \Psi_d^*(S_x, S_y)$

Image wave function $\Psi_i(x_i, y_i)$

$$\Psi_i(x_i, y_i) = \mathcal{F}^{-1}\,[\Psi_d(S_x, S_y)]$$

Image intensity $I_i(x_i, y_i)$

$$I_i(x_i, y_i) = \delta(0, 0) - 2\sigma v(x_i, y_i) * \mathcal{F}^{-1}\ [sin\ \gamma(S)]$$

Computed diffraction wave function $T(S_x, S_y)$

$$T(S_x, S_y) = \mathcal{F}\,[I_i(x_i, y_i)]$$
$$= \delta(0, 0) - 2\, F(S_x, S_y)\ sin\ \gamma(S)$$

400 kV image data of HSV-1 capsids

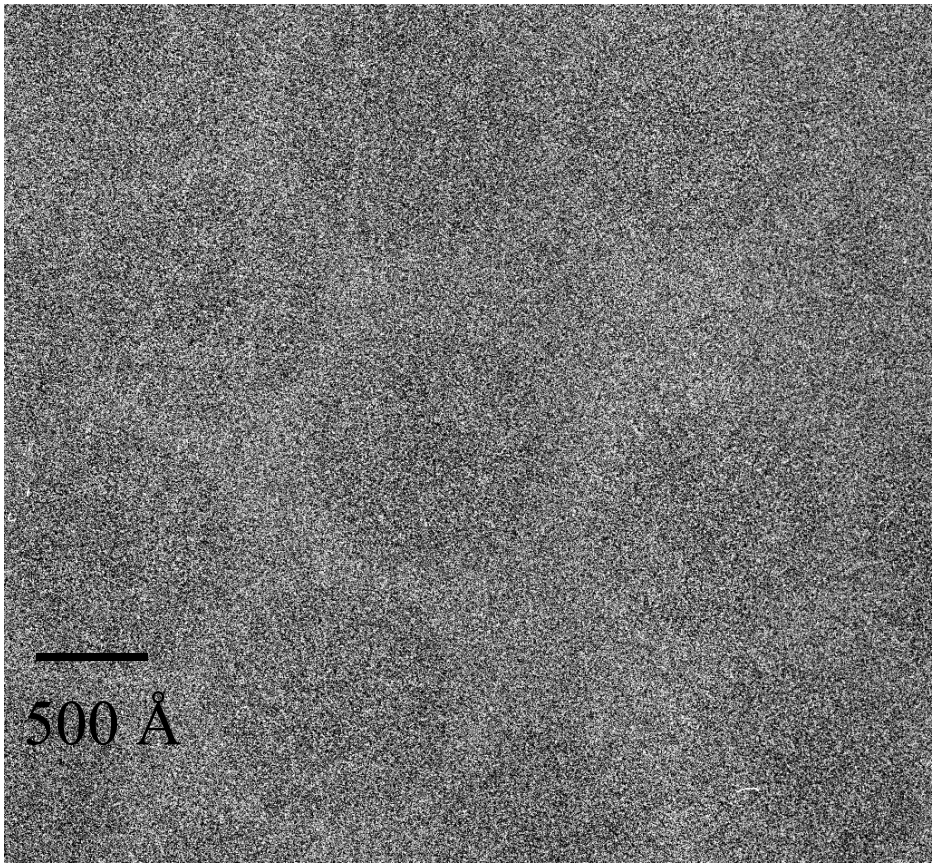

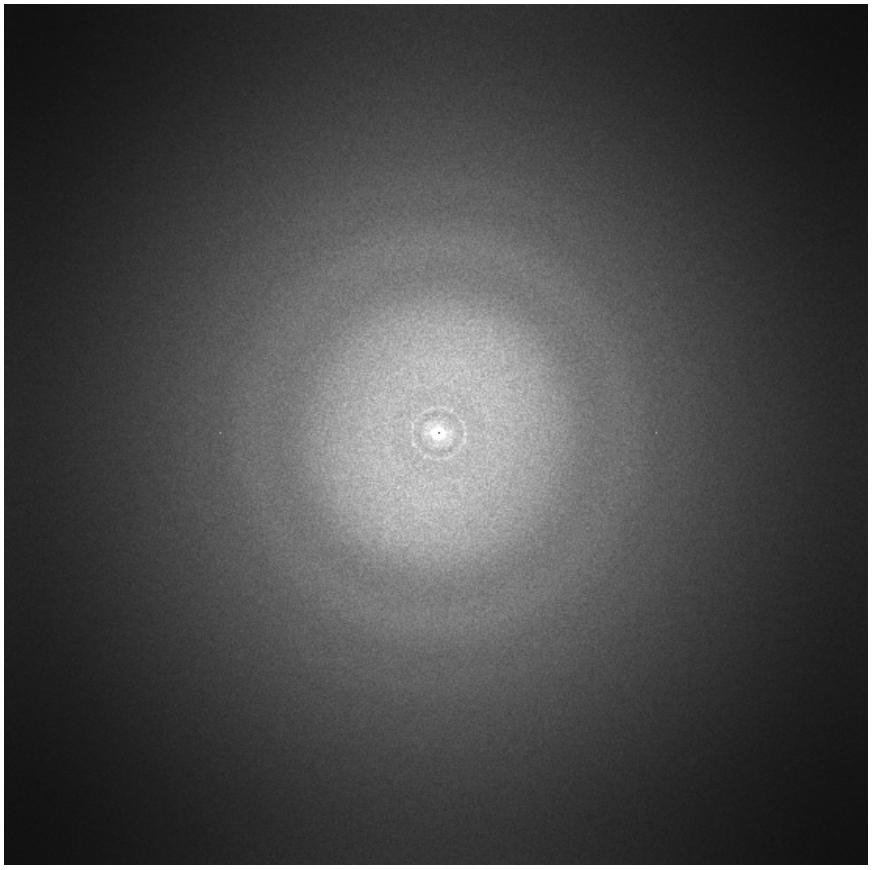

Joanita Jakana

Circularly Averaged Power Spectrum

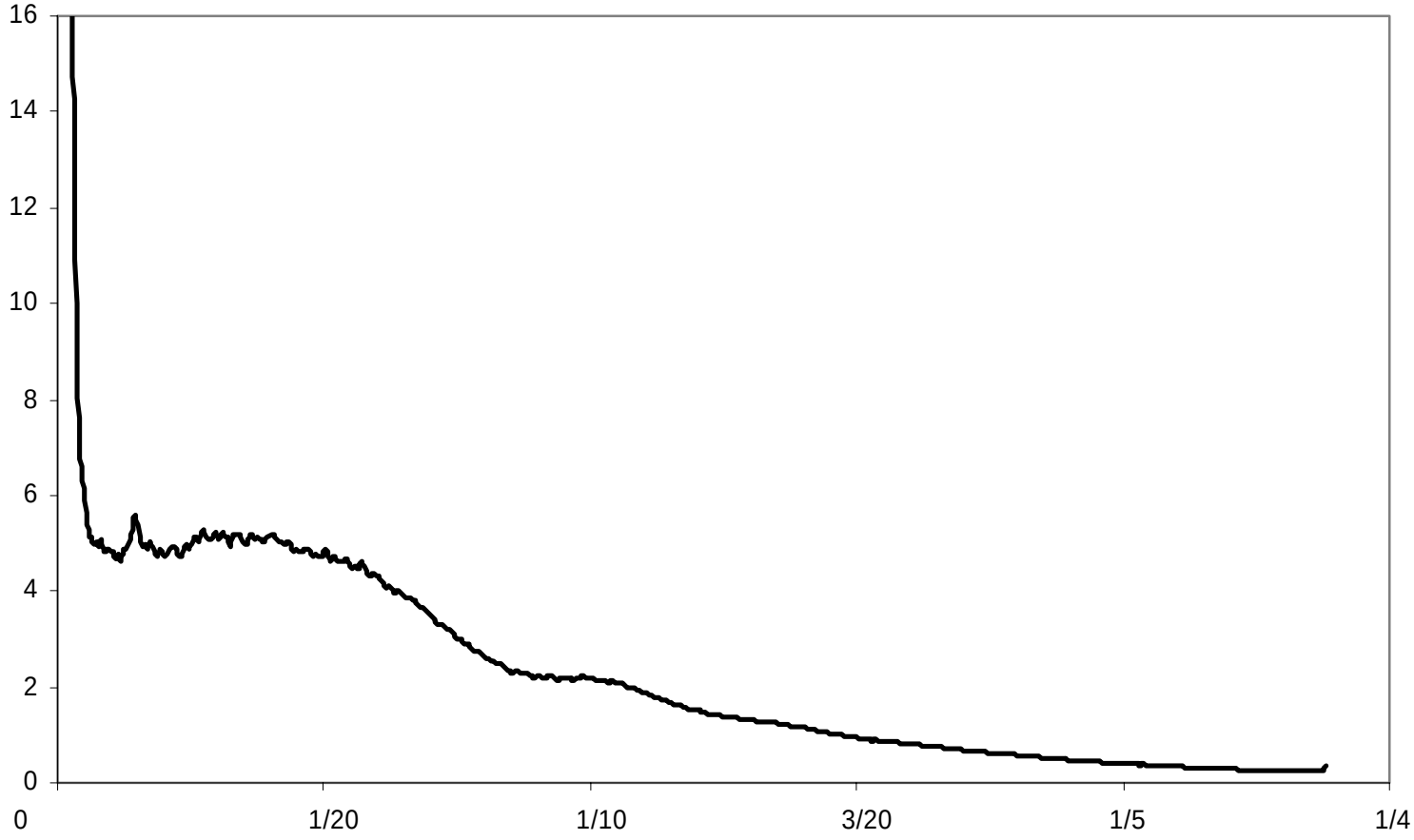

From Juan Chang and Joanita Jakana

Computed diffraction pattern

$$F^2(s)\ CTF^2(s)\ Env^2(s) + N^2(s)$$

Structure factor

Contrast transfer function

Envelope function

Background

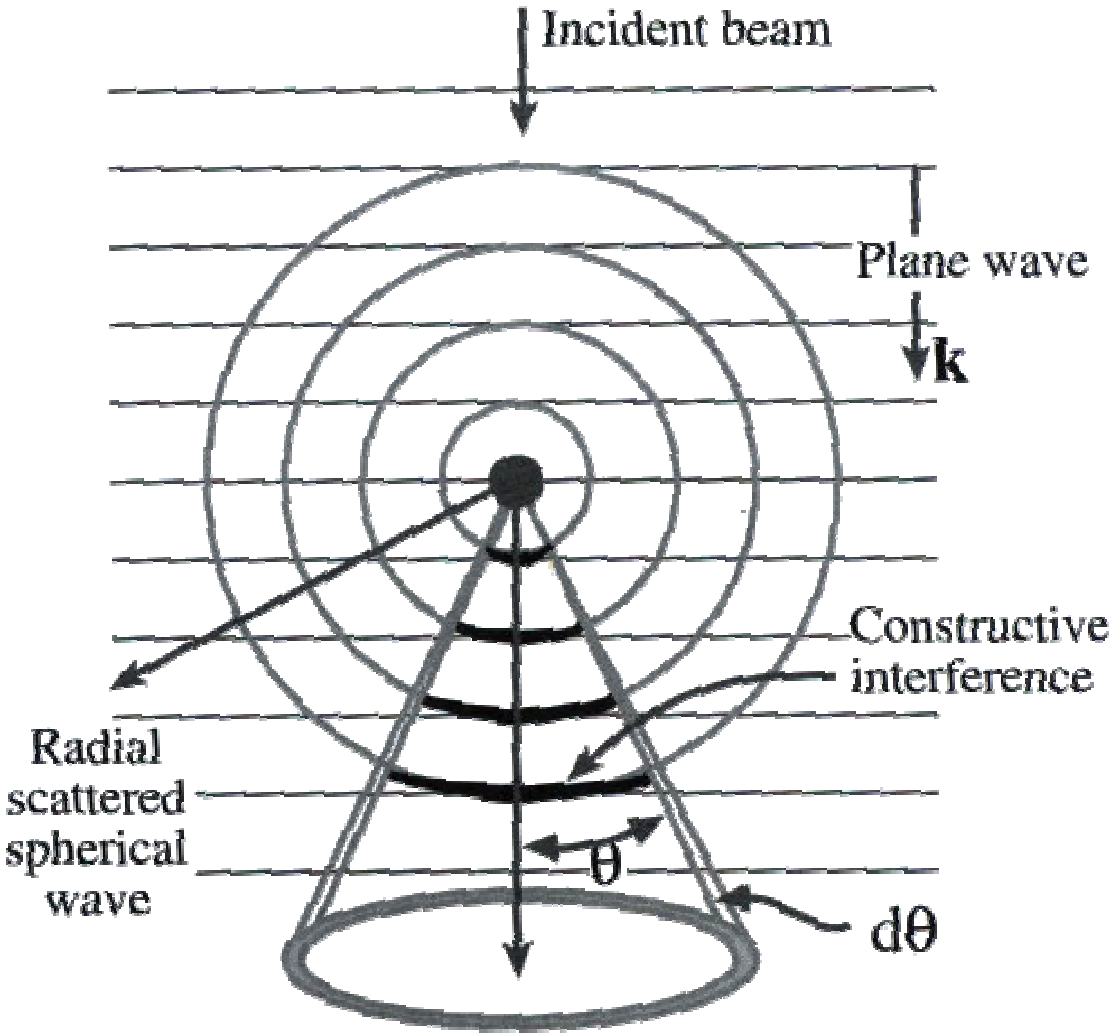

Figure 3.6. The generation of a scattered wave by the interaction of a plane wave (horizontal *lines*) with a point charge. The circles represent the scattered spherical wavefronts which are in phase (same λ). The in-phase constructive interference between the plane and spherical waves *is* shown by the dark arcs. The angles θ and $d\theta$ are the same as *in* Figure 2.3

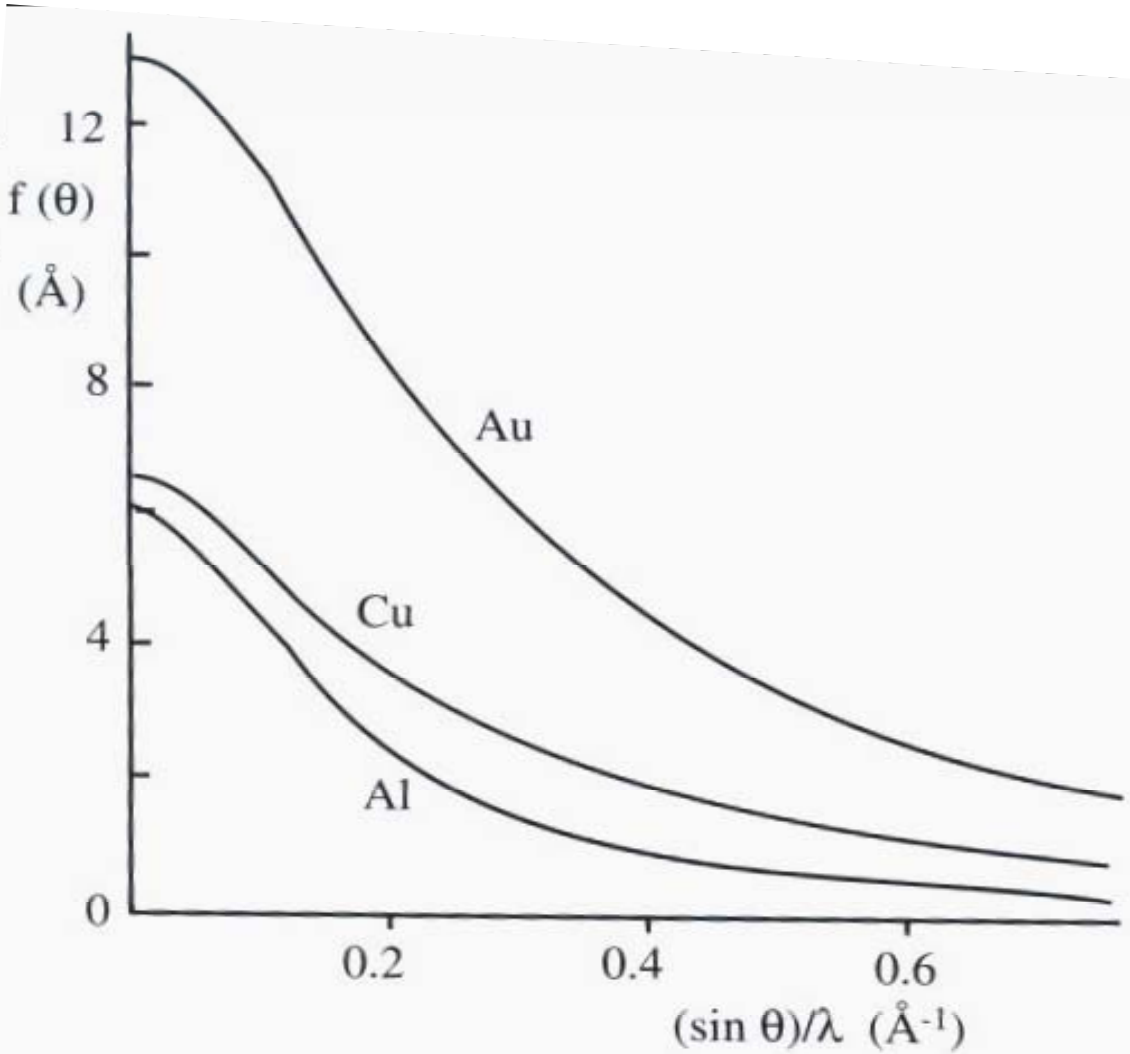

Figure 3.5. Change in the atomic scattering factor $f(\theta)$ with scattering angle θ (calculated from equation 3.10) showing that elastic scattering decreases with angle away from the incident beam direction ($\theta = 0°$) and increases with Z.

X-ray Scattering Intensity of HSV-1 Capsids

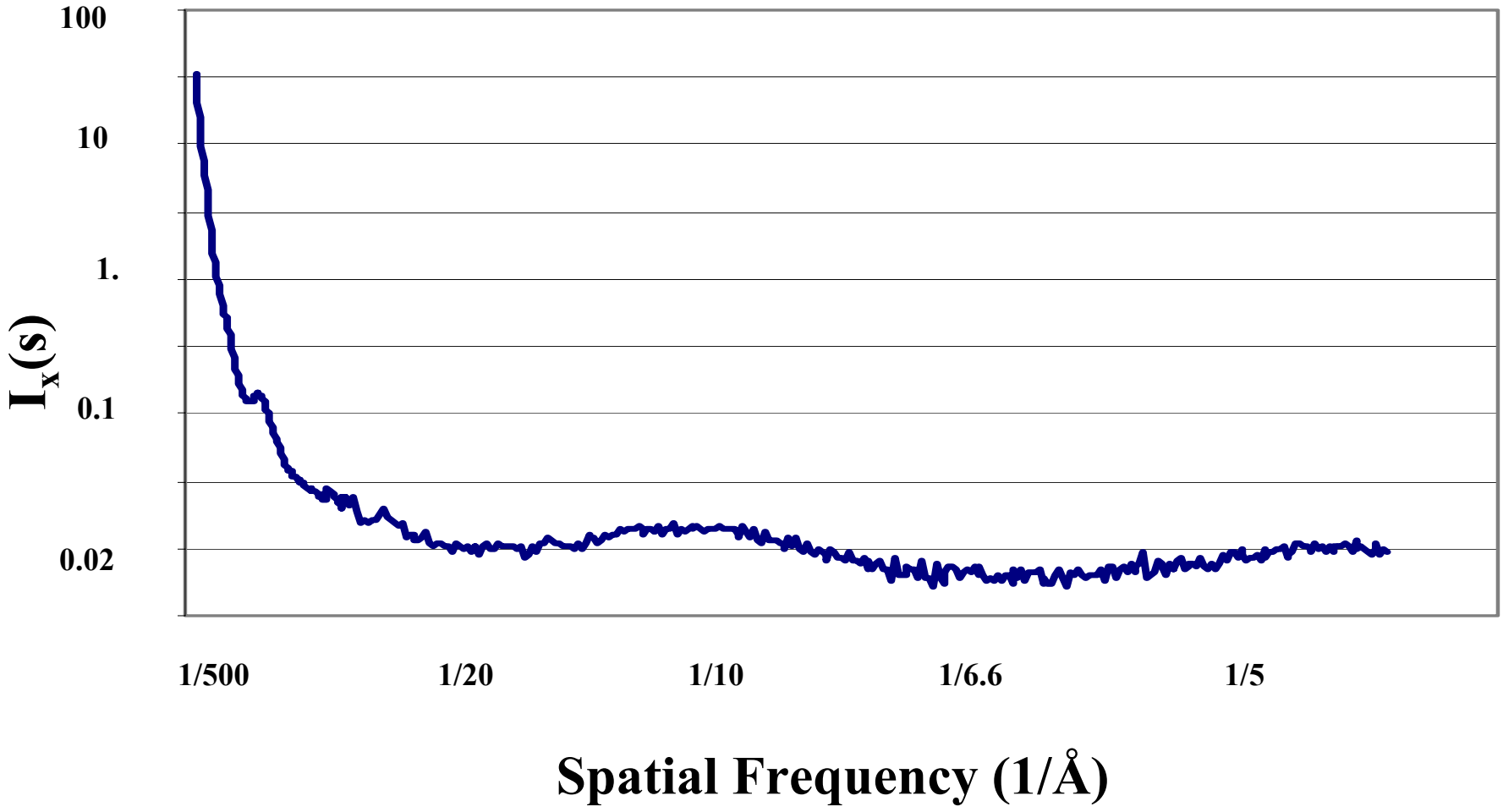

Dr. Hiro Tsuruta at SLAC

X ray Scattering Intensity of GroEL

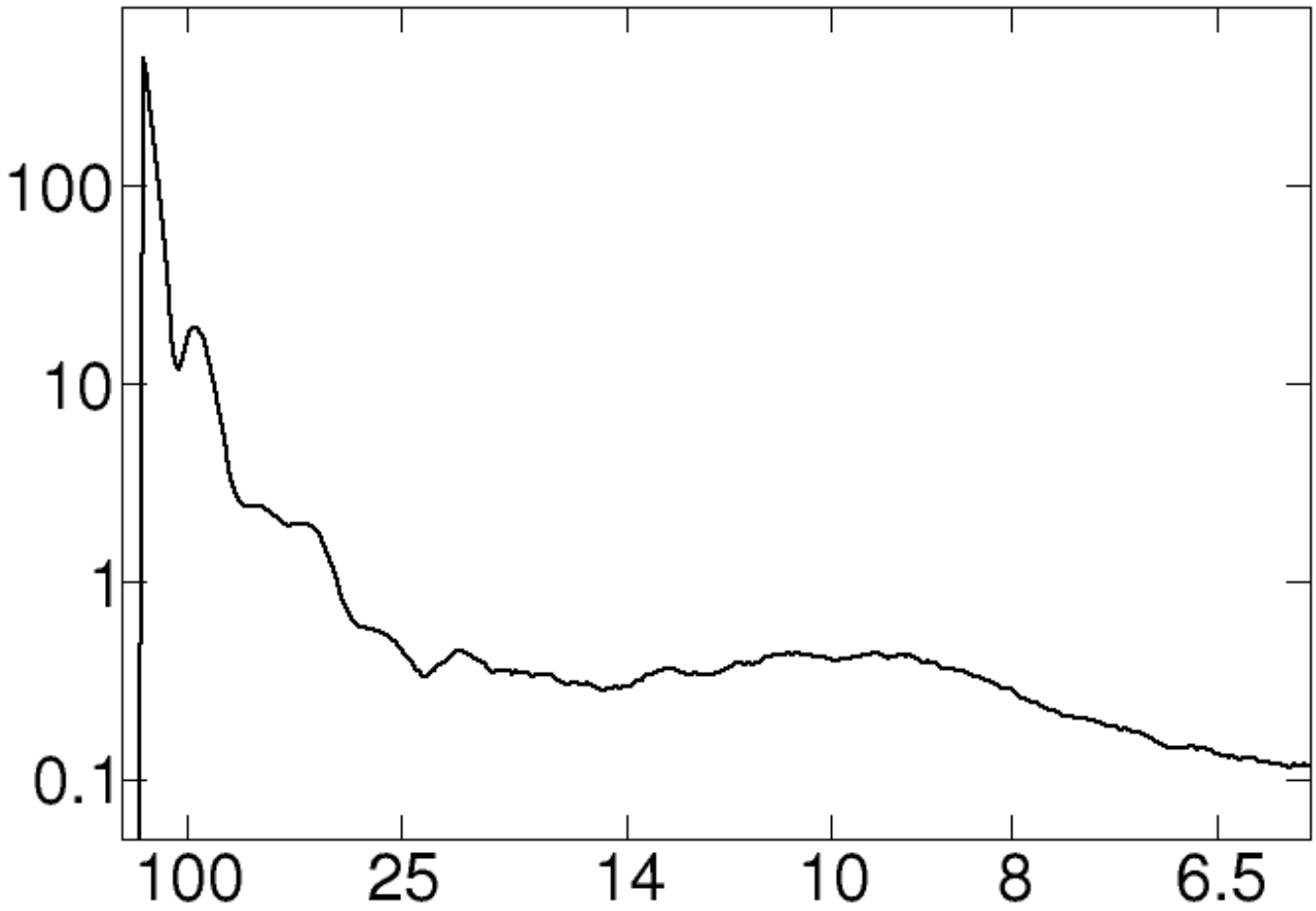

Resolution (Å)

Computed diffraction pattern

$$F^2(s)\ CTF^2(s)\ Env^2(s) + N^2(s)$$

Structure factor

Contrast transfer function

Envelope function

Background

Contrast Transfer Function

$$\mathrm{CTF}(s) = -A\left[(1-Q^2)^{1/2}\sin(\gamma) + Q\cos(\gamma)\right]$$

$$\gamma(s) = -2\pi\left(C_s\lambda^3 s^4/4 - \Delta Z\,\lambda s^2/2\right)$$

ΔZ is vector dependent if there is an astigmatism

CTF Simulation

Publication: Web-based Simulation for Contrast Transfer Function and Envelope Functions. Microscopy and Microanalysis 7(4), 329-334, 2001

Contrast of an ectron image is influenced by the contrast transfer function (CTF) and the envelope functions of the electron microscope. In order to plan an experimental condition for data collection or to interpret the contrast of an electron micrograph, one would often need to know the quantitative values of these functions for a given set of microscope parameters. This simulation program is written in Java applet and JavaScript programming language. The parameters of these functions can be adjusted interactively with slider bars and the plot for the simulated function would be updated instantaneously.

This applet is known to run on Windows (Netscape and Internet Explorer), Linux (i386) (Netscape), SGI IRIX (Netscape), OS/2 Warp and MacOS X. Please inform me if you found that this applet runs or has problems to run on other platforms.

The following is the detailed descriptions for some aspects of the applet page.

List of the special symbols/functions used in the applet

Term	Unit	Description
s	1/Å	resolution
v	keV	accelerating voltage
Cs	mm	spherical aberration

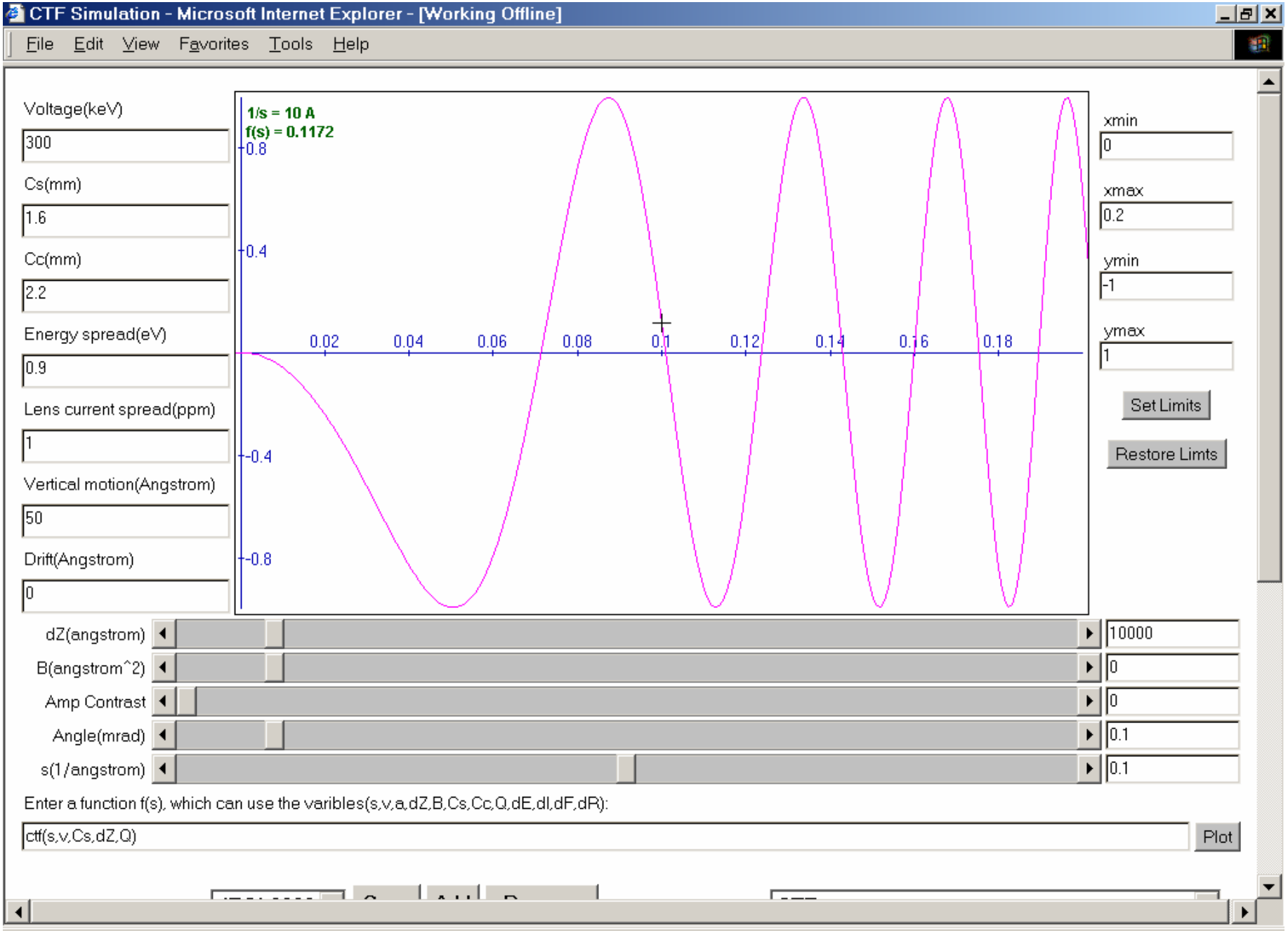
CTF Simulation - Microsoft Internet Explorer - [Working Offline]
File Edit View Favorites Tools Help
Voltage(keV)
300
Cs(mm)
1.6
Cc(mm)
2.2
Energy spread(eV)
0.9
Lens current spread(ppm)
1
Vertical motion(Angstrom)
50
Drift(Angstrom)
0
1/s = 10 A
f(s) = 0.1172
0.8
0.4
-0.4
-0.8
0.02
0.04
0.06
0.08
0.1
0.12
0.14
0.16
0.18
xmin
0
xmax
0.2
ymin
-1
ymax
1
Set Limits
Restore Limts
dZ(angstrom)
10000
B(angstrom^2)
0
Amp Contrast
0
Angle(mrad)
0.1
s(1/angstrom)
0.1
Enter a function f(s), which can use the varibles(s,v,a,dZ,B,Cs,Cc,Q,dE,dI,dF,dR):
ctf(s,v,Cs,dZ,Q)
Plot

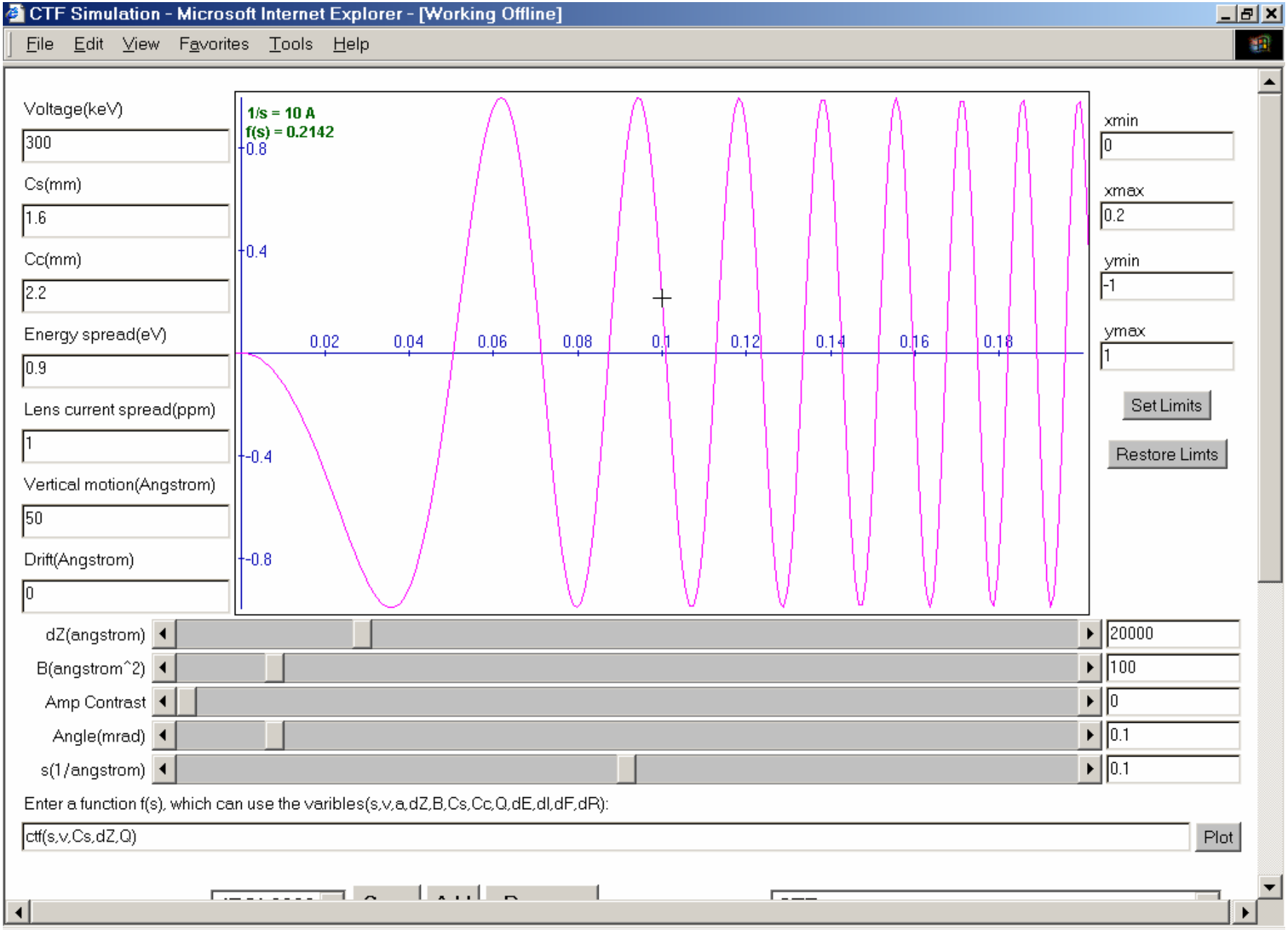
CTF Simulation - Microsoft Internet Explorer - [Working Offline]
File Edit View Favorites Tools Help
Voltage(keV)
300
Cs(mm)
1.6
Cc(mm)
2.2
Energy spread(eV)
0.9
Lens current spread(ppm)
1
Vertical motion(Angstrom)
50
Drift(Angstrom)
0
1/s = 10 A
f(s) = 0.2142
0.8
0.4
-0.4
-0.8
0.02
0.04
0.06
0.08
0.1
0.12
0.14
0.16
0.18
xmin
0
xmax
0.2
ymin
-1
ymax
1
Set Limits
Restore Limts
dZ(angstrom)
20000
B(angstrom^2)
100
Amp Contrast
0
Angle(mrad)
0.1
s(1/angstrom)
0.1
Enter a function f(s), which can use the varibles(s,v,a,dZ,B,Cs,Cc,Q,dE,dI,dF,dR):
ctf(s,v,Cs,dZ,Q)
Plot

Astigmatism

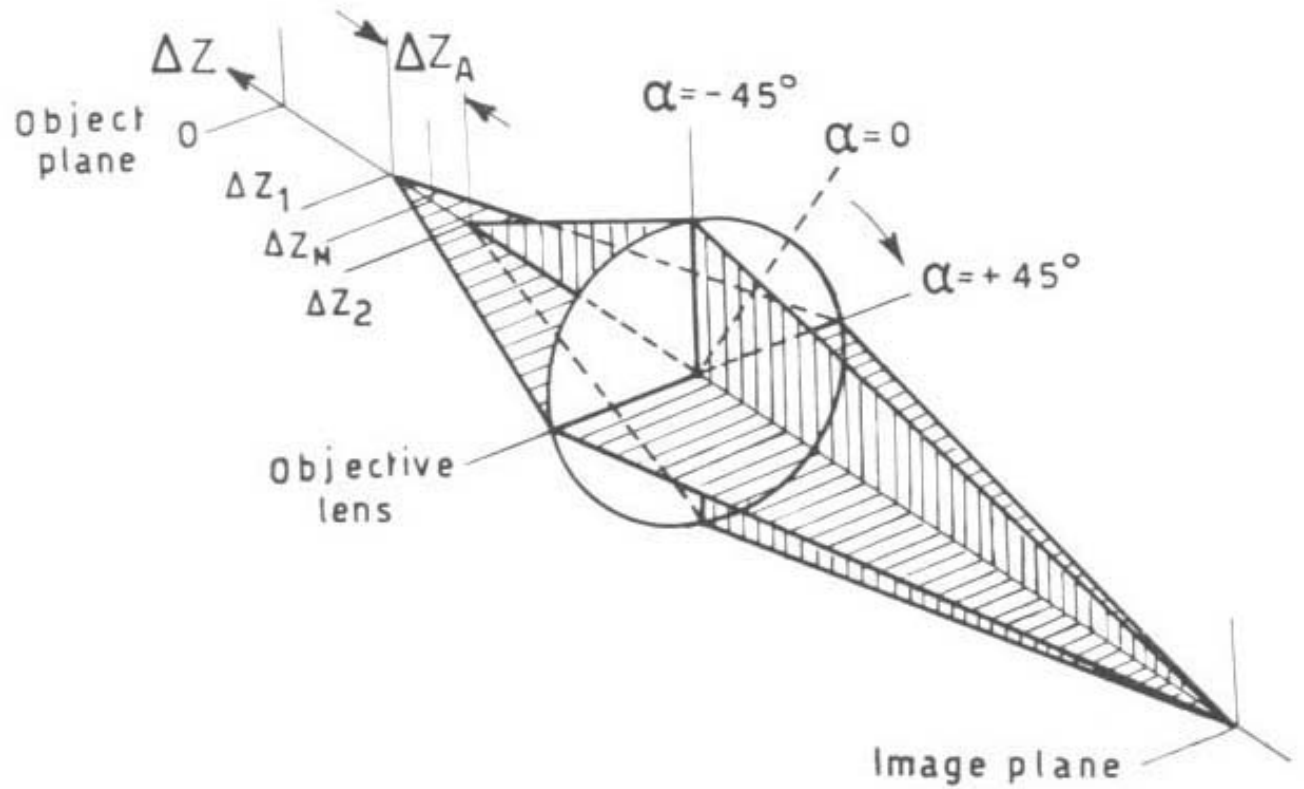

From F. Thon

Astigmatism

$$\Delta Z_{eff}(\alpha) = \Delta Z_m + (\Delta Z_a \sin 2\alpha)/2$$

$$\Delta Z_m = (\Delta Z_1 + \Delta Z_2)/2$$

$$\Delta Z_a = \Delta Z_1 - \Delta Z_2$$

Synthetic Power Spectrum $\Delta Z = 0.8\mu m$

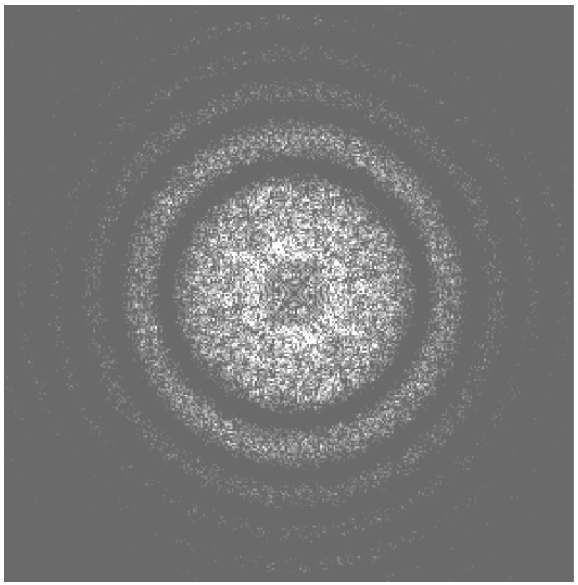

Astigmatism amplitude = 0.0µm

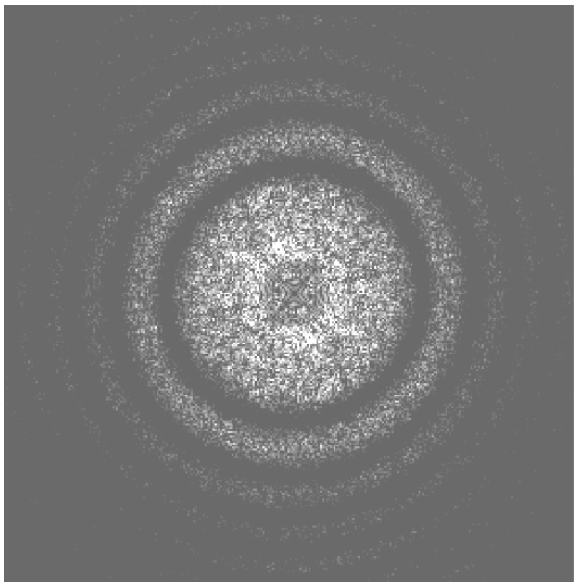

Astigmatism amplitude = 0.0267µm

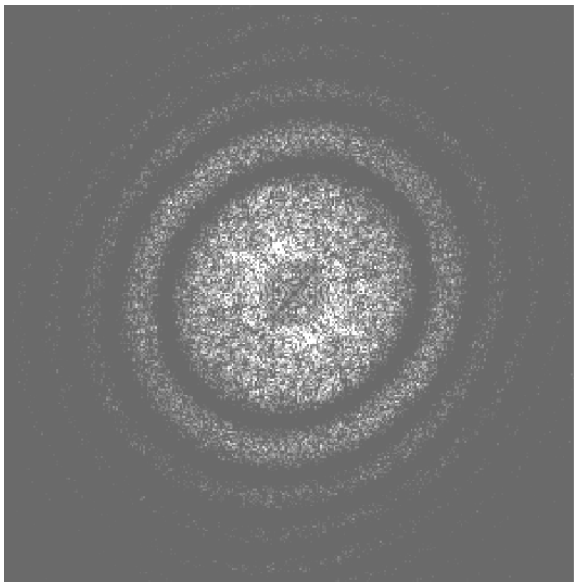

Astigmatism amplitude = 0.1µm

From Wen Jiang

Synthetic Power Spectrum $\Delta Z = 3\ \mu m$

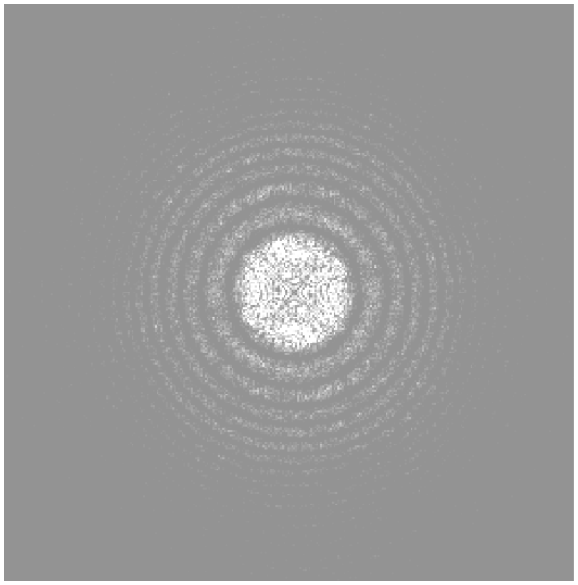

Astigmatism amplitude = 0.0µm

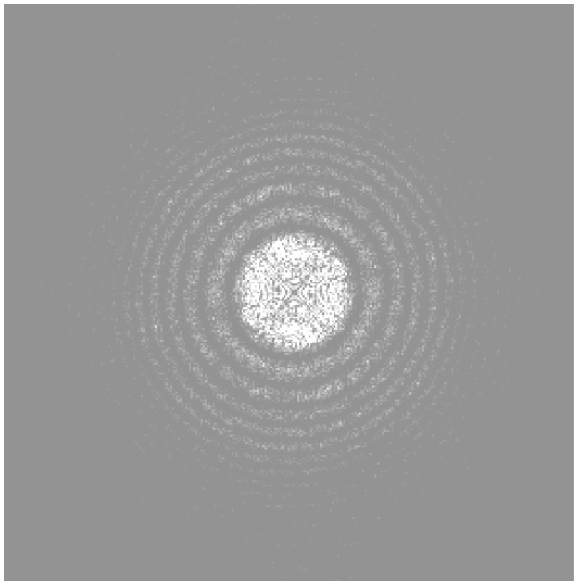

Astigmatism amplitude = 0.1µm

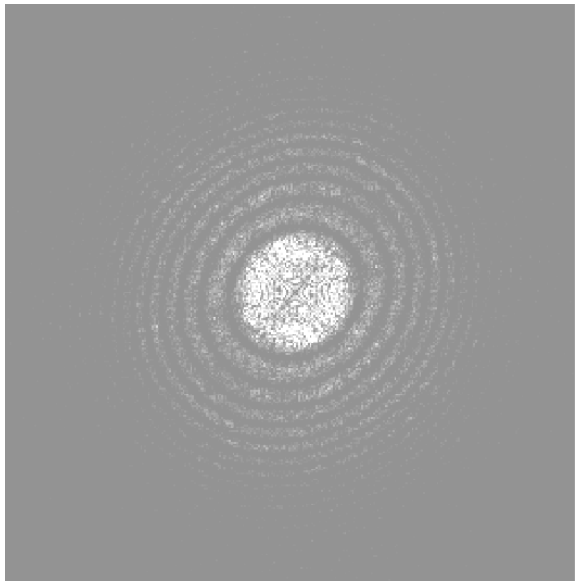

Astigmatism amplitude = 0.375µm

From Wen Jiang

Astigmatism in Single Particle Image

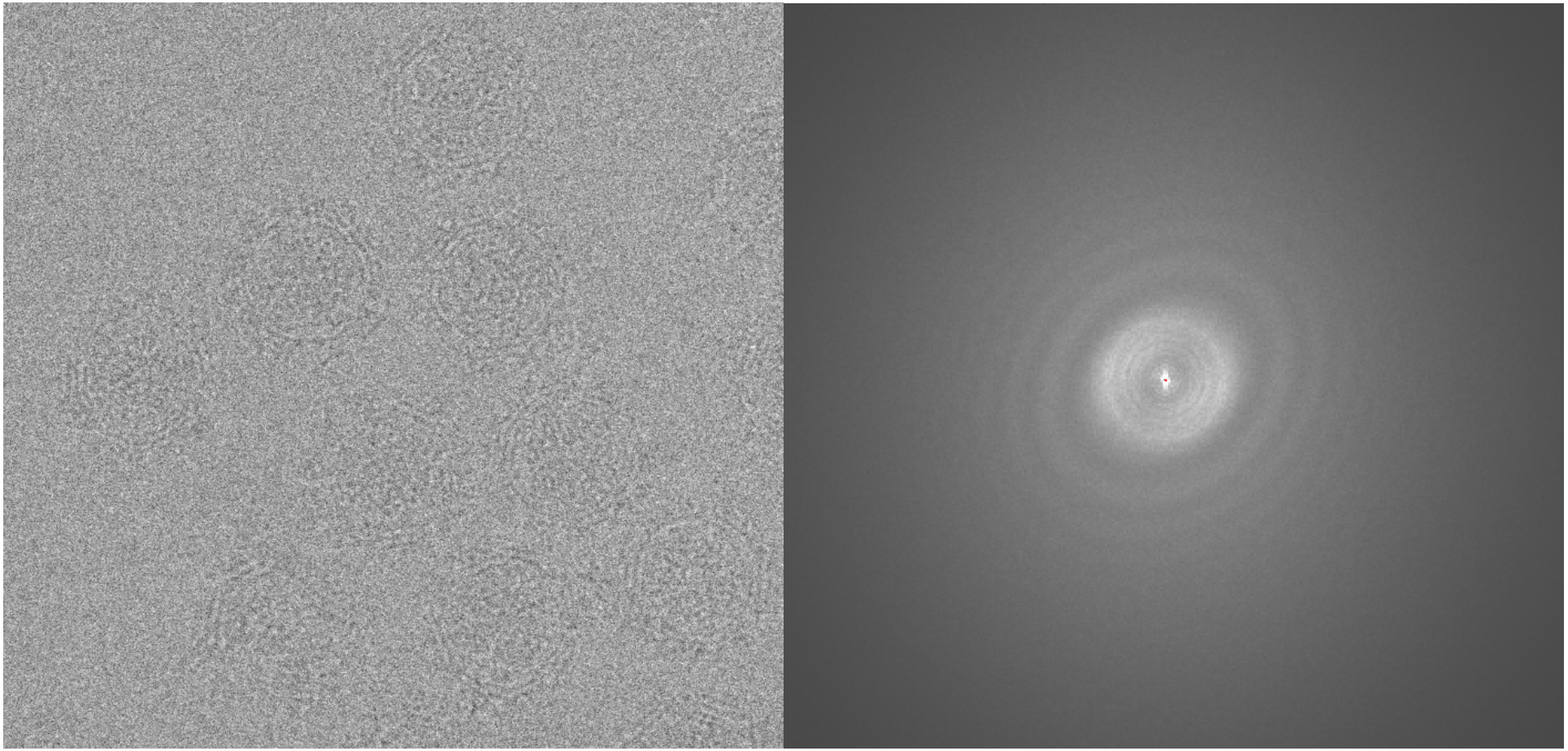

From Dr. Angel Paredes

Computed diffraction pattern

$$F^2(s)\ \ CTF^2(s)\ \ Env^2(s) + N^2(s)$$

Structure factor

Contrast transfer function

Envelope function

Background

EM Envelope Functions : Env(s)

Gaussian type source:

$$G_{sc}(s) = \exp[-\pi^2 \alpha^2 (C_S \lambda^2 s^3 - \Delta Z s)^2]$$

Gaussian type fluctuation:

$$G_{tc}(s) = \exp[-\frac{\pi^2}{16 \ln 2} C_C^2 \lambda^2 (\frac{\Delta E}{E})^2 s^4]$$

Gaussian type fluctuation:

$$G_{ol}(s) = \exp[-\frac{\pi^2}{4 \ln 2} C_C^2 \lambda^2 (\frac{\Delta I}{I})^2 s^4]$$

Sinusoidal type fluctuation:

$$G_{lm}(s) = J_O(\pi \Delta f \lambda s^2)$$

Drift:

$$G_{tm}(s) = \frac{\sin(\pi s \Delta r)}{\pi s \Delta r}$$

Spatial coherence envelope function

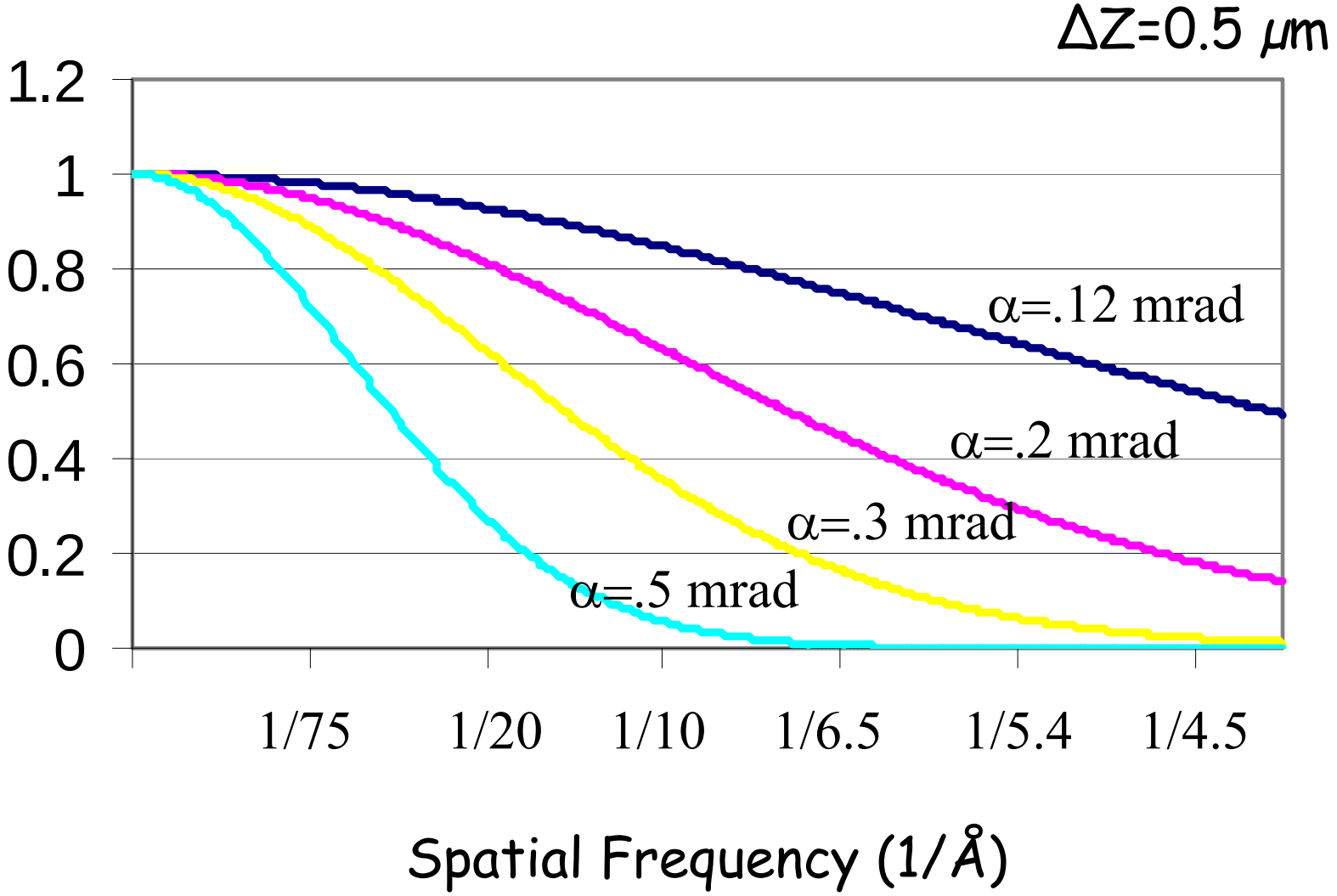

300 keV, *Cs* = 1.6 mm, defocus = 1 μM

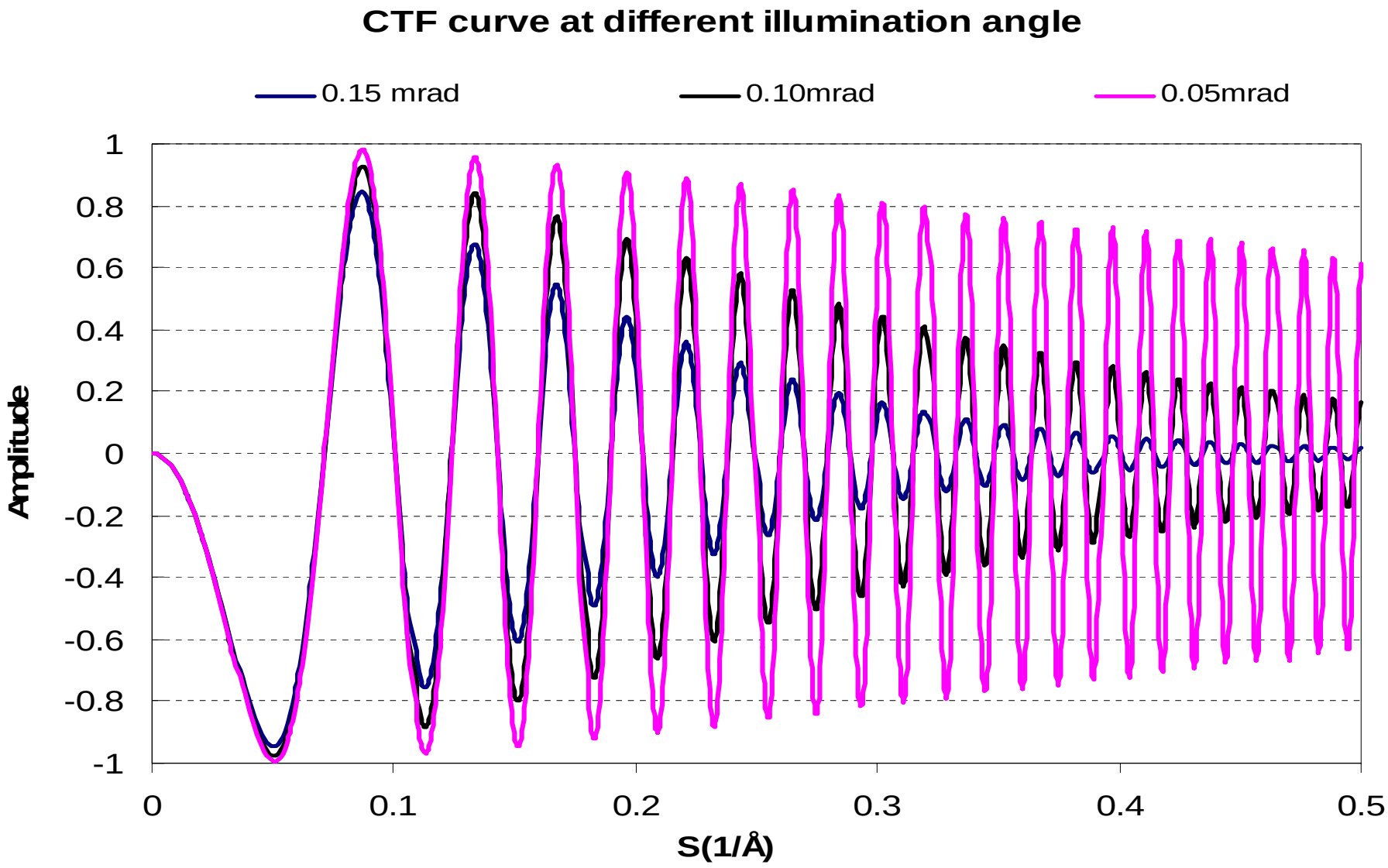

EM Envelope Functions : Env(s)

Gaussian type source:

$$G_{sc}(s) = \exp[-\pi^2 \alpha^2 (C_S \lambda^2 s^3 - \Delta Z s)^2]$$

Gaussian type fluctuation:

$$G_{tc}(s) = \exp[-\frac{\pi^2}{16 \ln 2} C_C^2 \lambda^2 (\frac{\Delta E}{E})^2 s^4]$$

Gaussian type fluctuation:

$$G_{ol}(s) = \exp[-\frac{\pi^2}{4 \ln 2} C_C^2 \lambda^2 (\frac{\Delta I}{I})^2 s^4]$$

Sinusoidal type fluctuation:

$$G_{lm}(s) = J_O(\pi \Delta f \lambda s^2)$$

Drift:

$$G_{tm}(s) = \frac{\sin(\pi s \Delta r)}{\pi s \Delta r}$$

Gaussian Approximation for Cumulative Envelope Function

$$Env^2(s) \sim \exp(-2BS^2)$$

Fitting the spatial coherence envelope function with exp(-BS²)

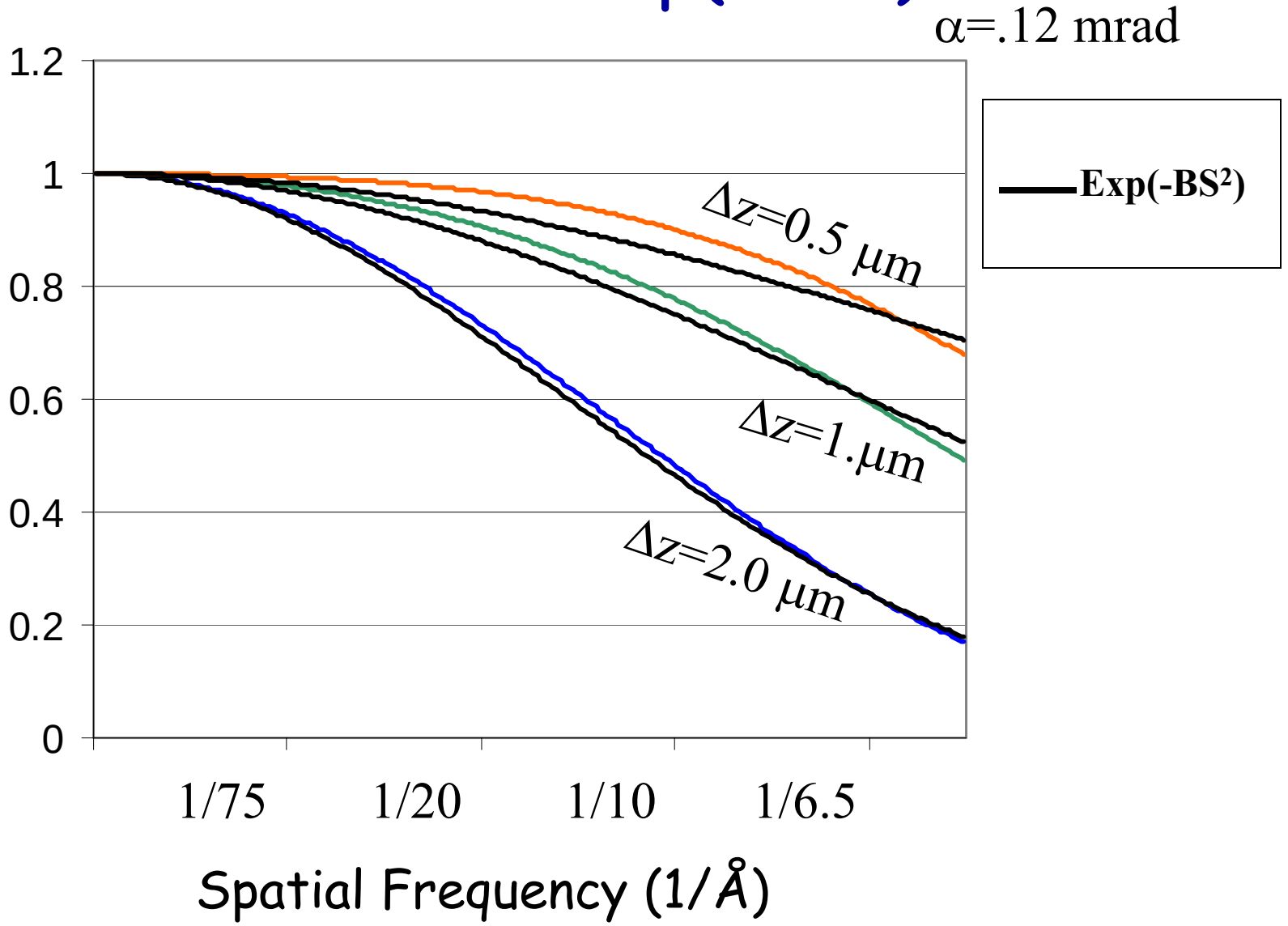

Computed diffraction pattern

$$F^2(s)\ CTF^2(s)\ Env^2(s) + N^2(s)$$

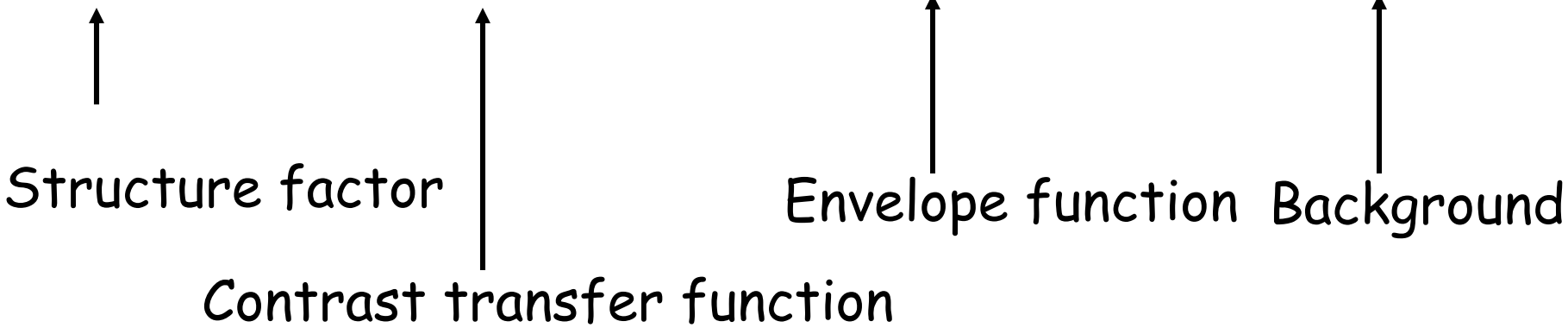

Noise Function

$$N^2(s) = n_1 \exp(n_2 s + n_3 s^2 + n_4 s^{1/2})$$

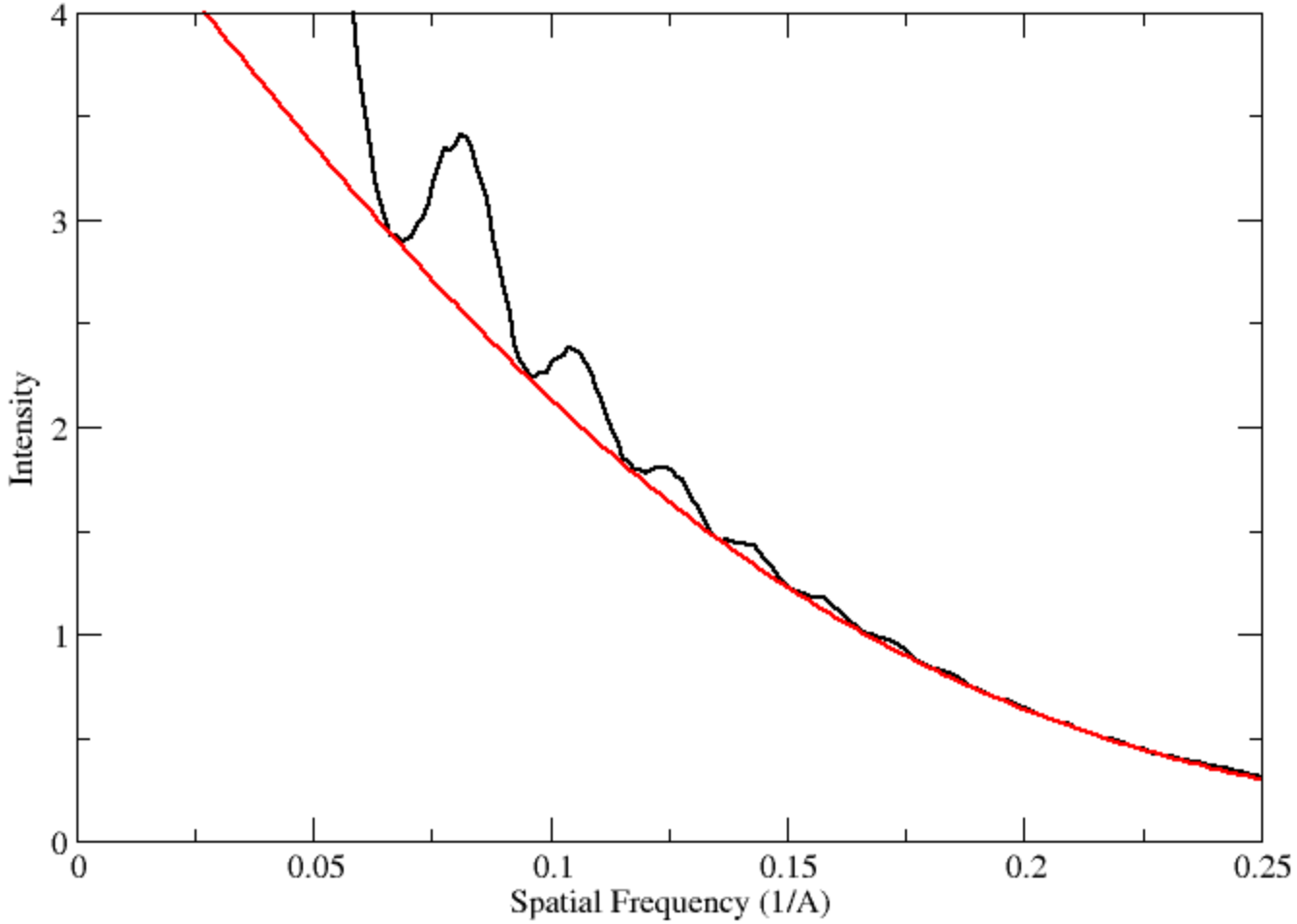

From Dr. Z. Li

$$\text{Contrast} = (F^2 \ \ CTF^2 \ \ E^2 \ ) \ / \ N^2$$

200kV Image and Power Spectrum of CPV

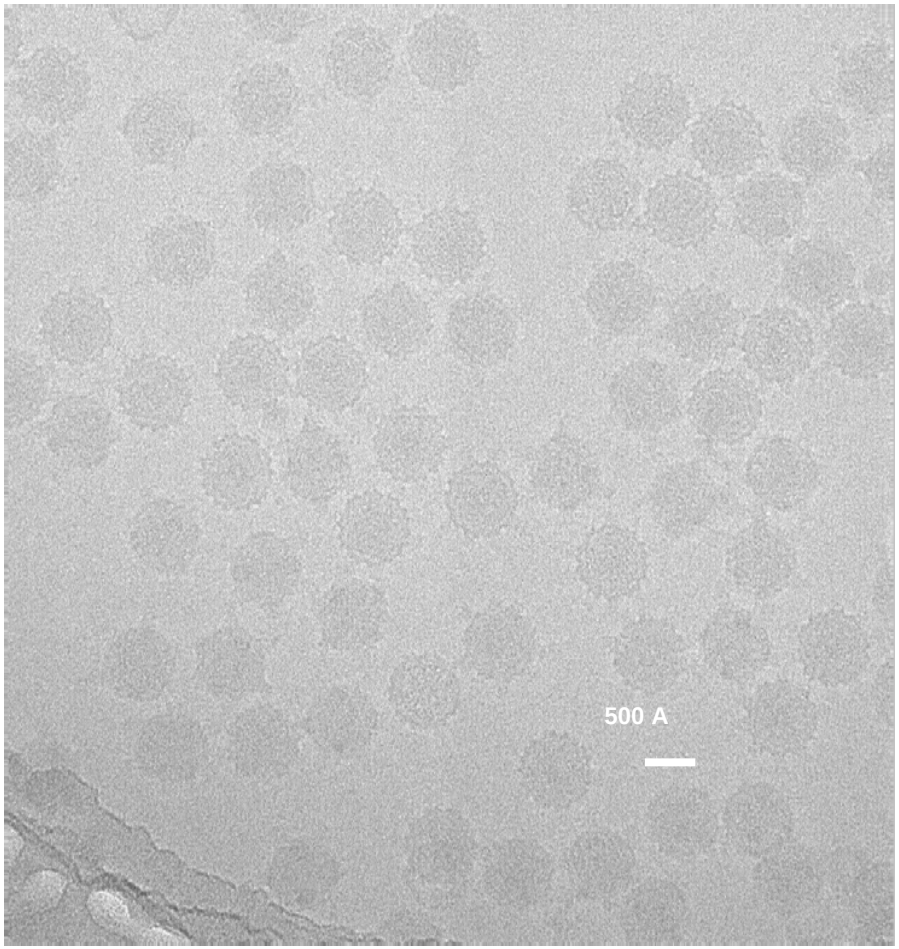

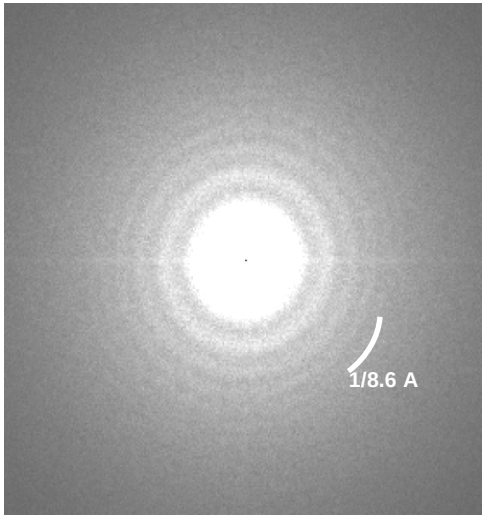

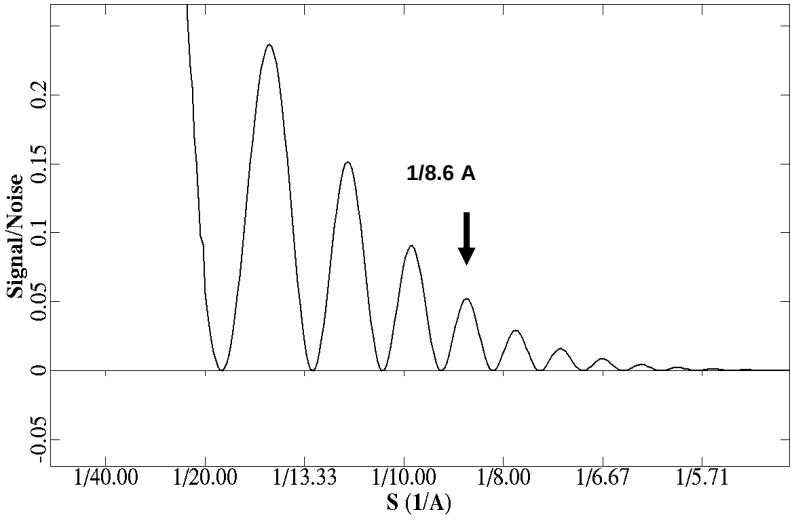

Booth JSB 2004

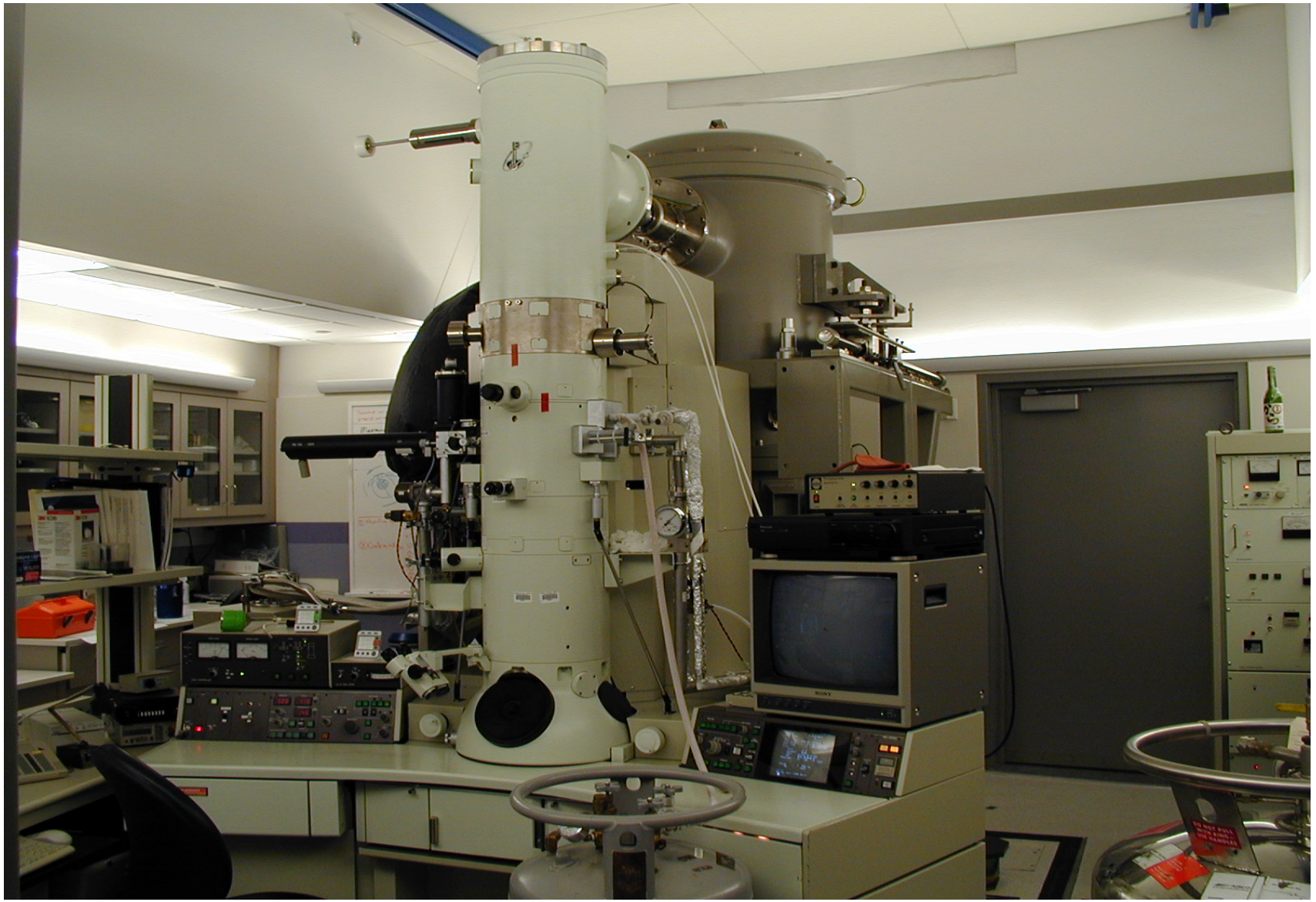

JEOL 3000SFF electron cryomicroscope at NCMI
equipped with liquid helium stage and field emission gun

300kV CPV Image

Power Spectrum

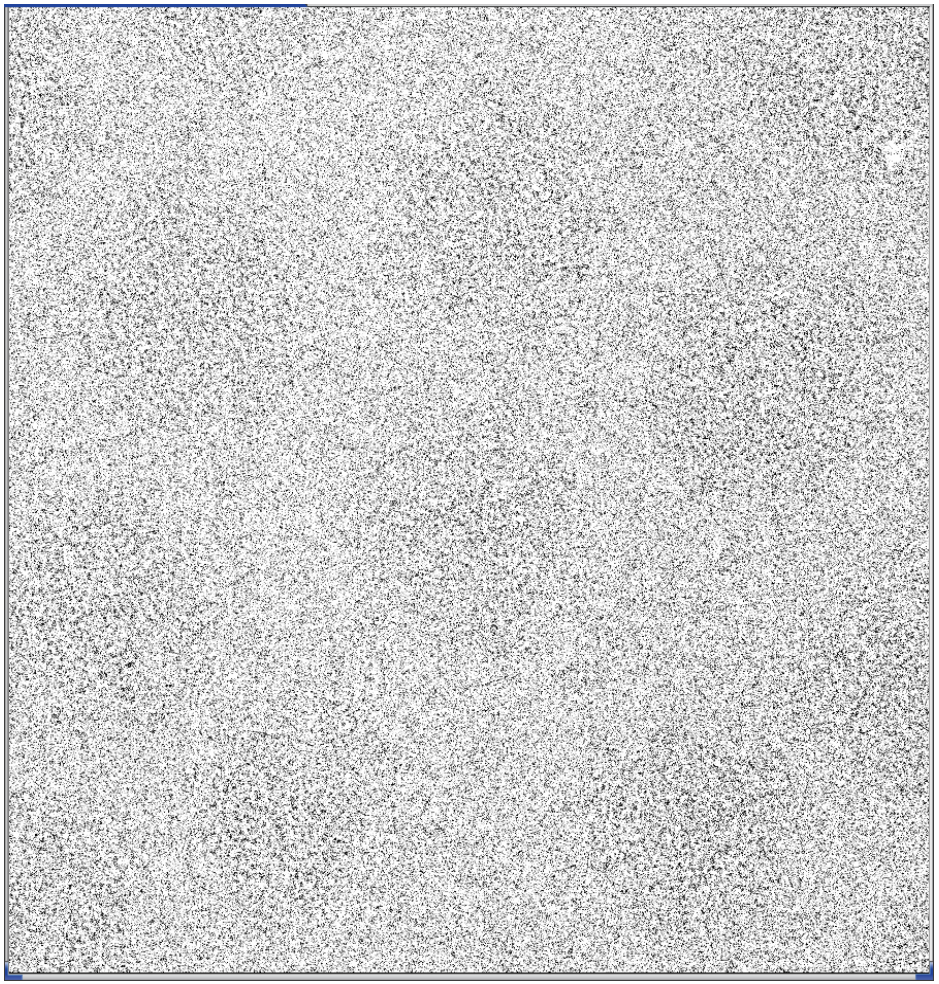

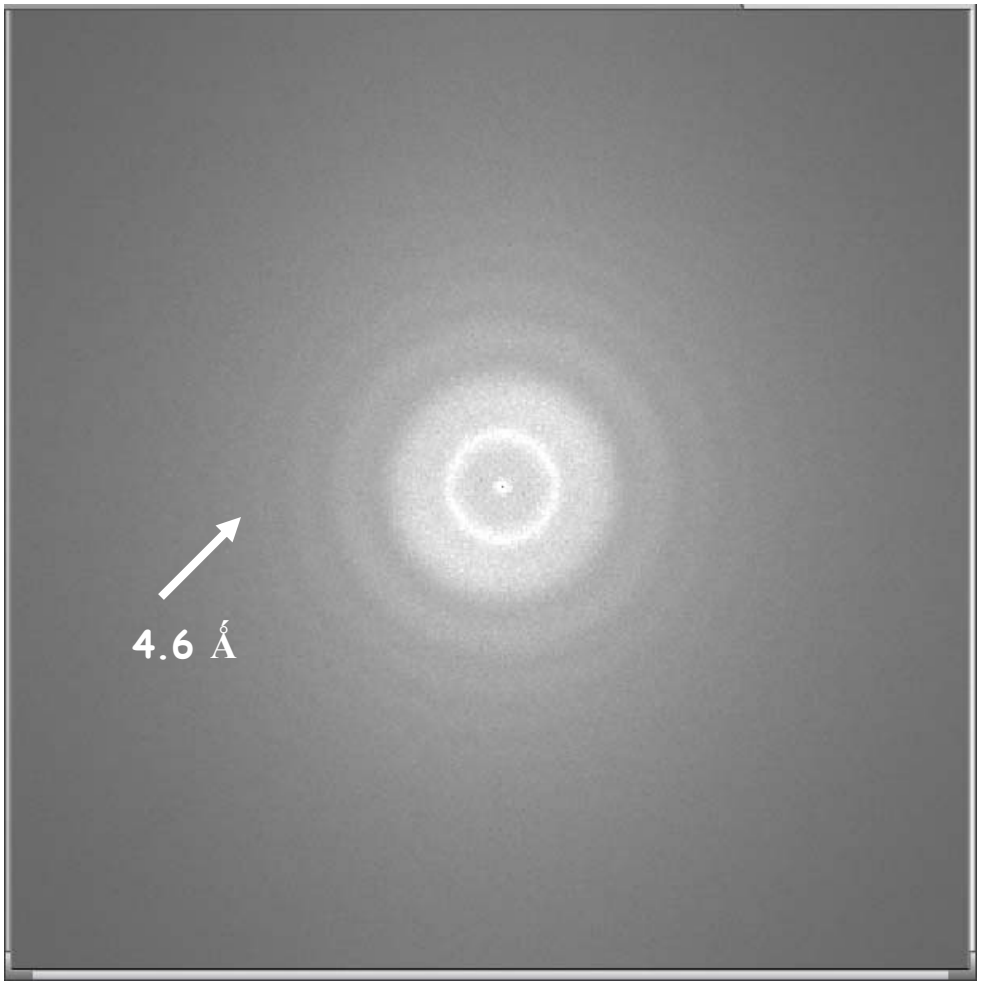

156 particles, ΔZ = 0.60 μm
Joanita Jakana, MSA Proceeding, 2004

Experimental B factor vs defocus for 300 kV Images of CPV

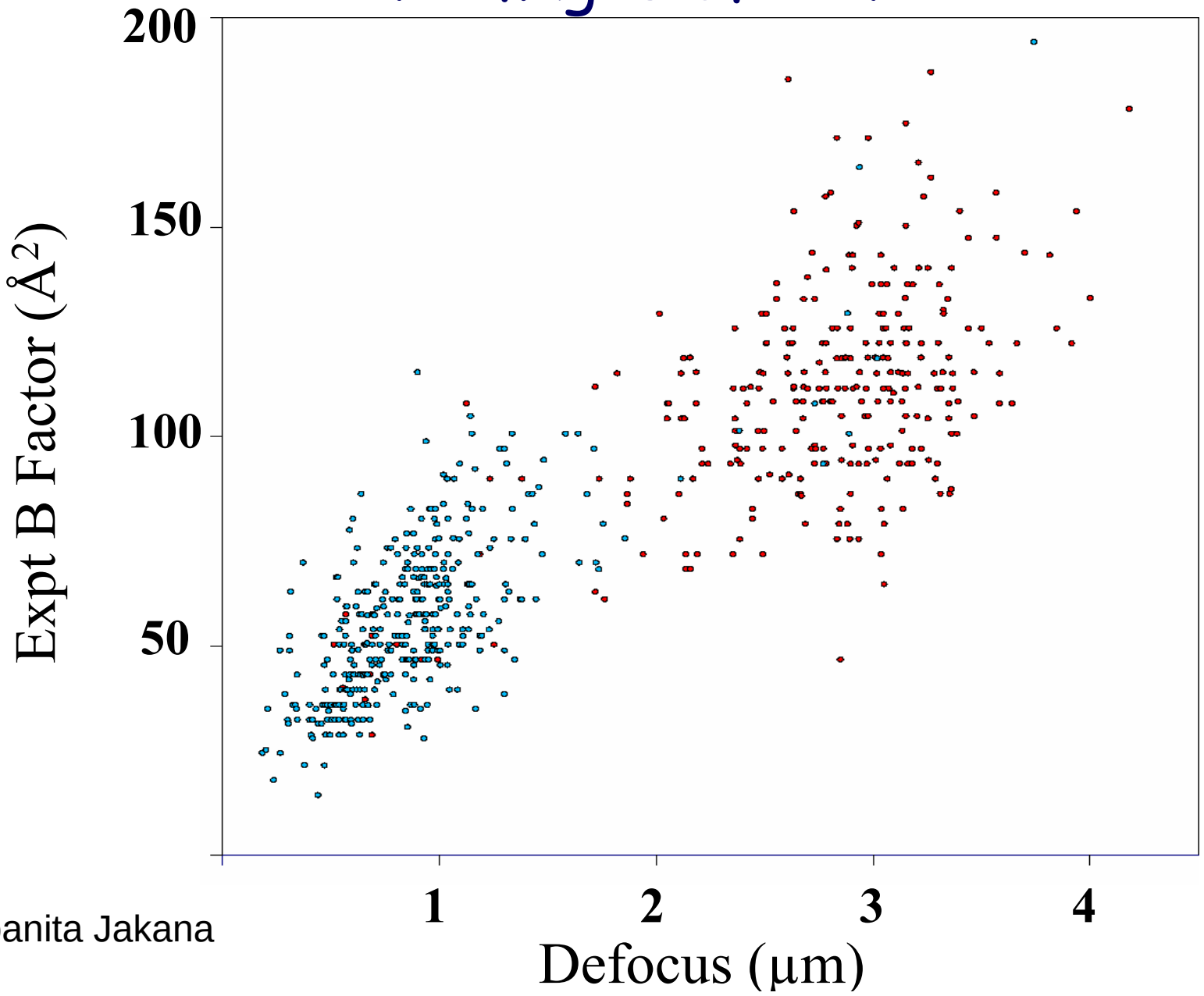

Joanita Jakana

Number of particles

required for a 3-D reconstruction is inversely proportional to

$$F^2(S)\ \exp(-2BS^2)$$

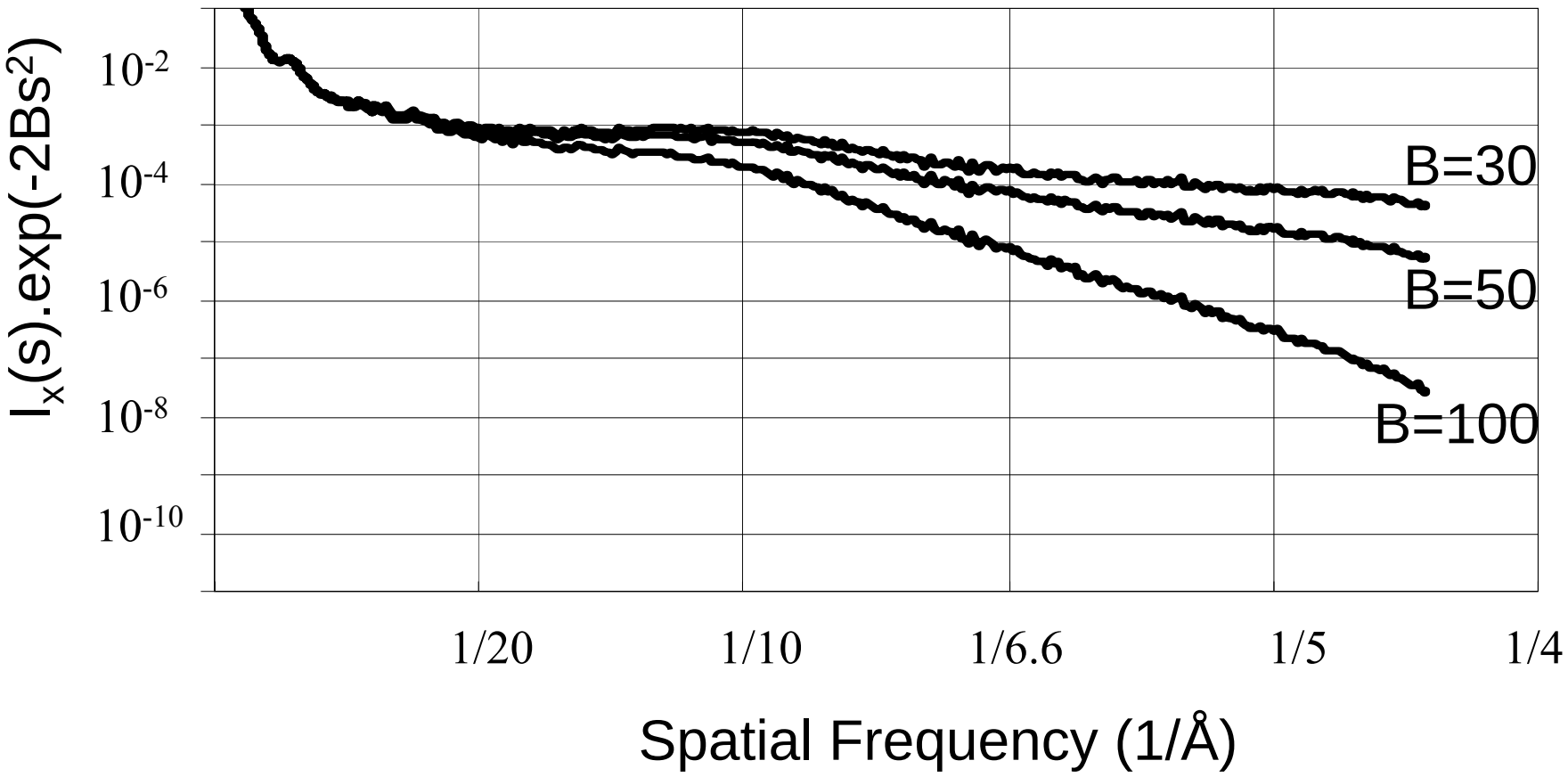
$I_x(s).\exp(-2Bs^2)$
10^{-2}
10^{-4}
10^{-6}
10^{-8}
10^{-10}
B=30
B=50
B=100
1/20
1/10
1/6.6
1/5
1/4
Spatial Frequency (1/Å)

Causes of High B-Factor

- Large angle of illumination (defocus dependent)
- Astigmatism (defocus independent)
- Local specimen movement (defocus independent)
- Insufficient sampling (defocus independent)

Synthetic Power Spectrum $\Delta Z = 0.8\mu m$

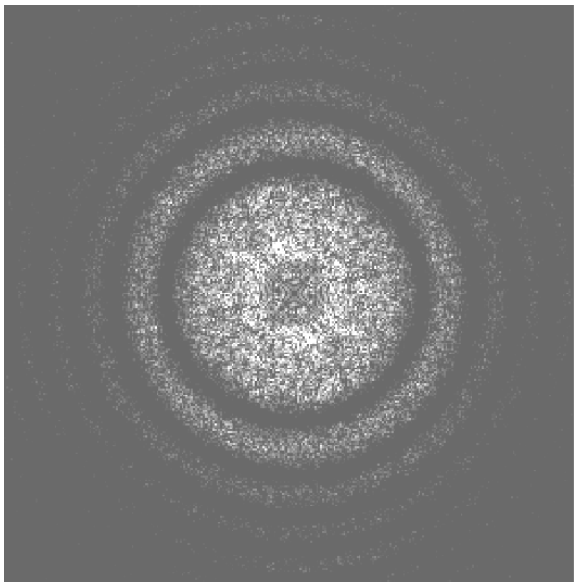

Astigmatism amplitude = 0.0µm

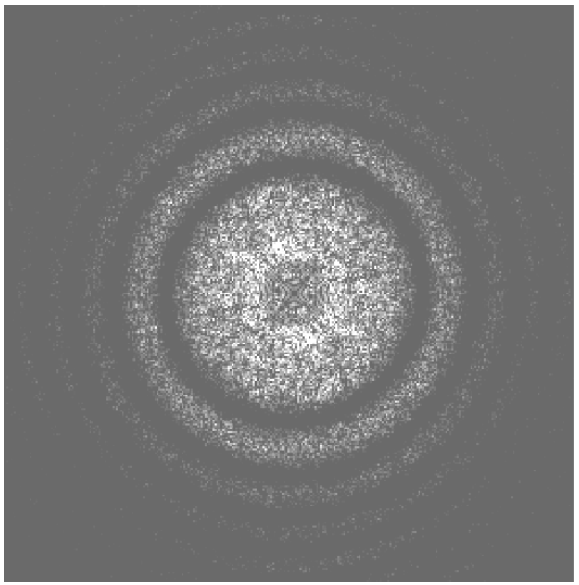

Astigmatism amplitude = 0.0267µm

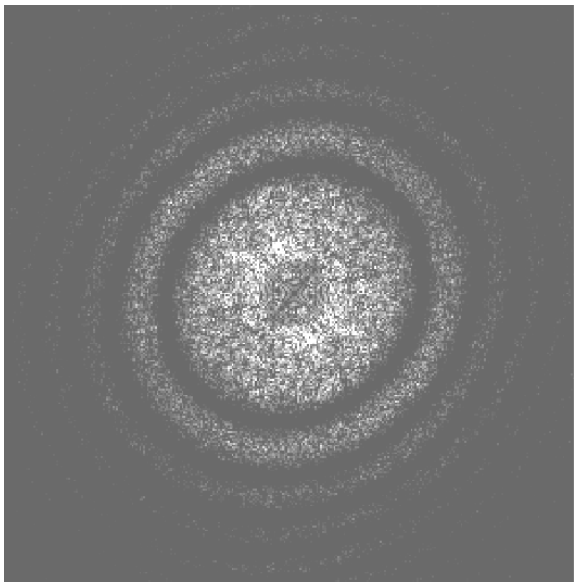

Astigmatism amplitude = 0.1µm

From Wen Jiang

300kV, Cs=1.6mm

ΔZ=0.8 μm astigmatism = 0.0 μm, 0.0267 μm, 0.1μm

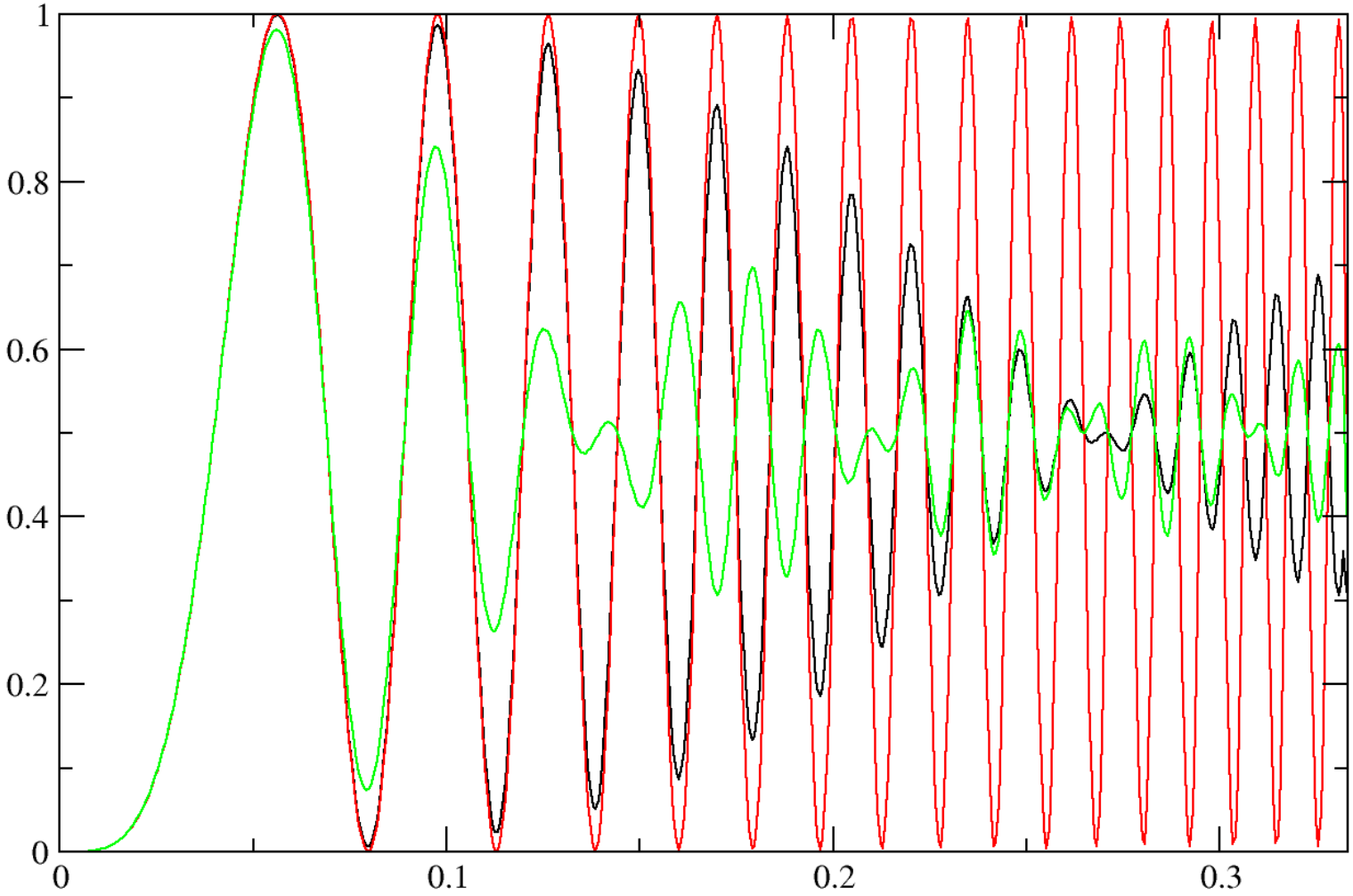

Sampling

- Sampling distance in real space :

  $\Delta x = \frac{1}{2}$ - 1/3 expected resolution

- Sampling distance in Fourier space

  $\Delta S = 1/(N\ \Delta x)$

- Choice of sampling (Δx) and box size (N) depends on expected resolution and the defocus used

Shannon - Nyquist sampling and aliasing.

Hence if object density contains fine details out to a spatial frequency $\frac{1}{2d}$ (ie spatial period $2d$) then sampling must not be coarser than d, otherwise neighbouring copies of the periodic transform begin to overlap. If the overlap were severe, high frequency terms from one copy of the transform overlap and contaminate low frequencies of the next. ie high frequencies would masquerade as low ones. This is known as <u>aliasing</u>.

coarsely sampled object

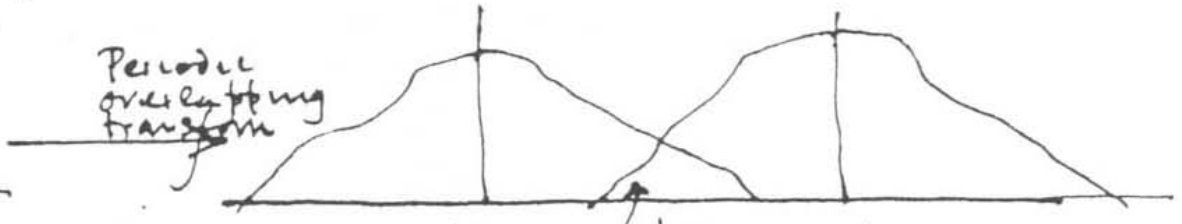

hi frequency components overlap lower frequency components.

From T Crowther

Effect of Particle Size on CTF Appearance

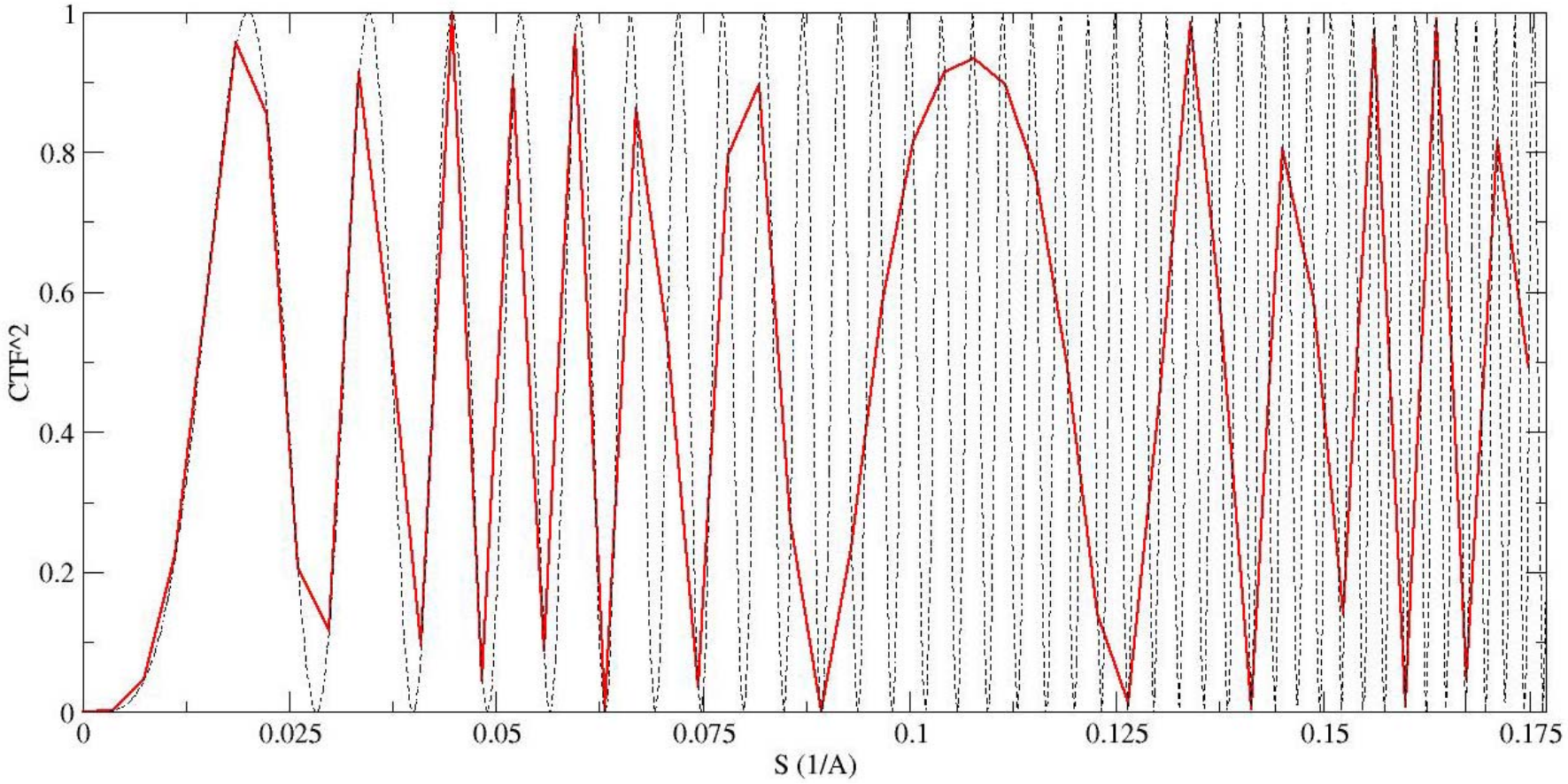

200 kV, *Cs* = 1.2mm, 2.8 *A*/pixel. 96x96 pixels box, ΔZ=5 μm

Effect of Particle Size on CTF Appearance

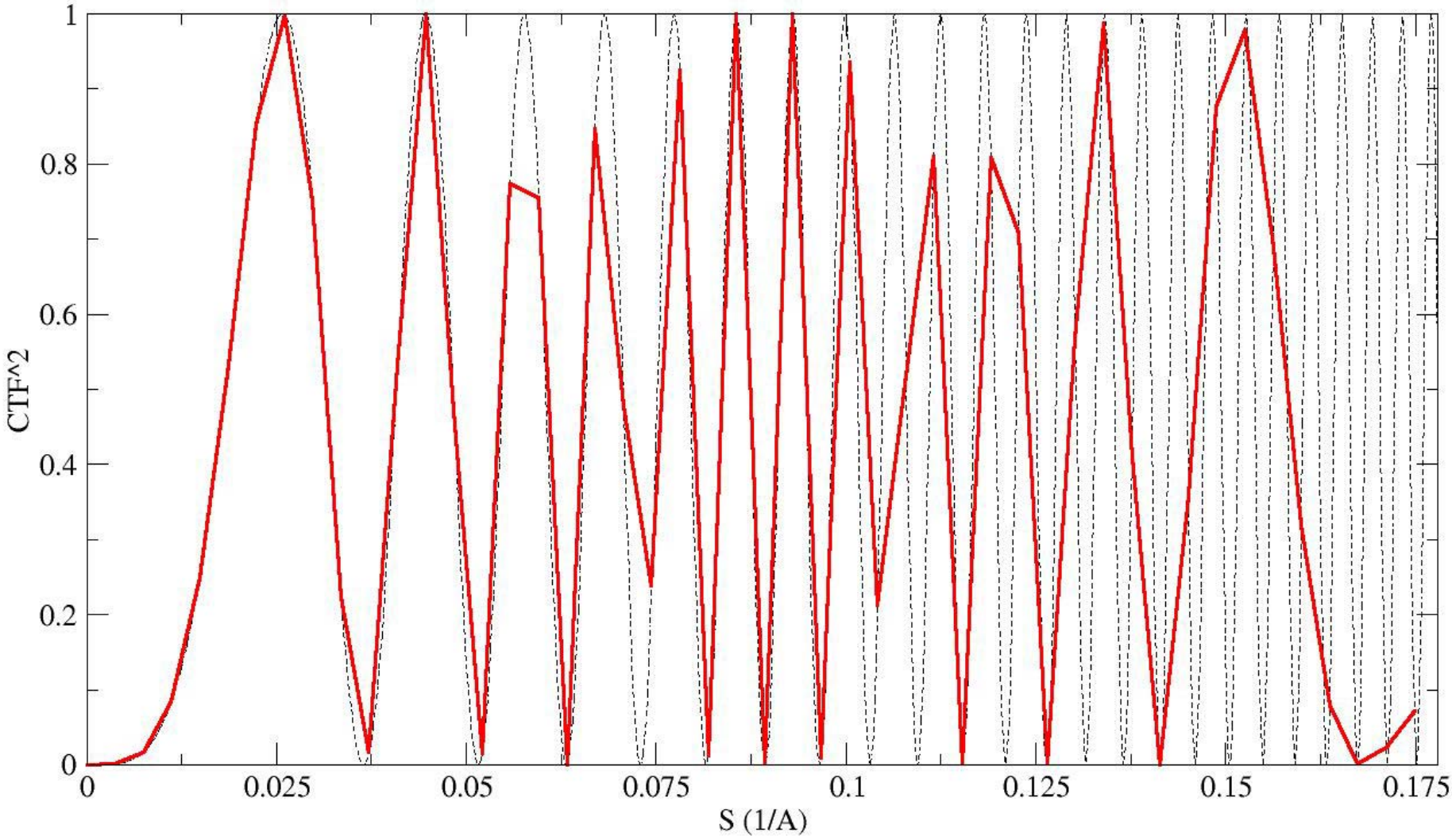

200 kV, *Cs* = 1.2mm, 2.8 *A*/pixel. 96x96 pixels box, ΔZ=3 µm

Effect of Particle Size on CTF Appearance

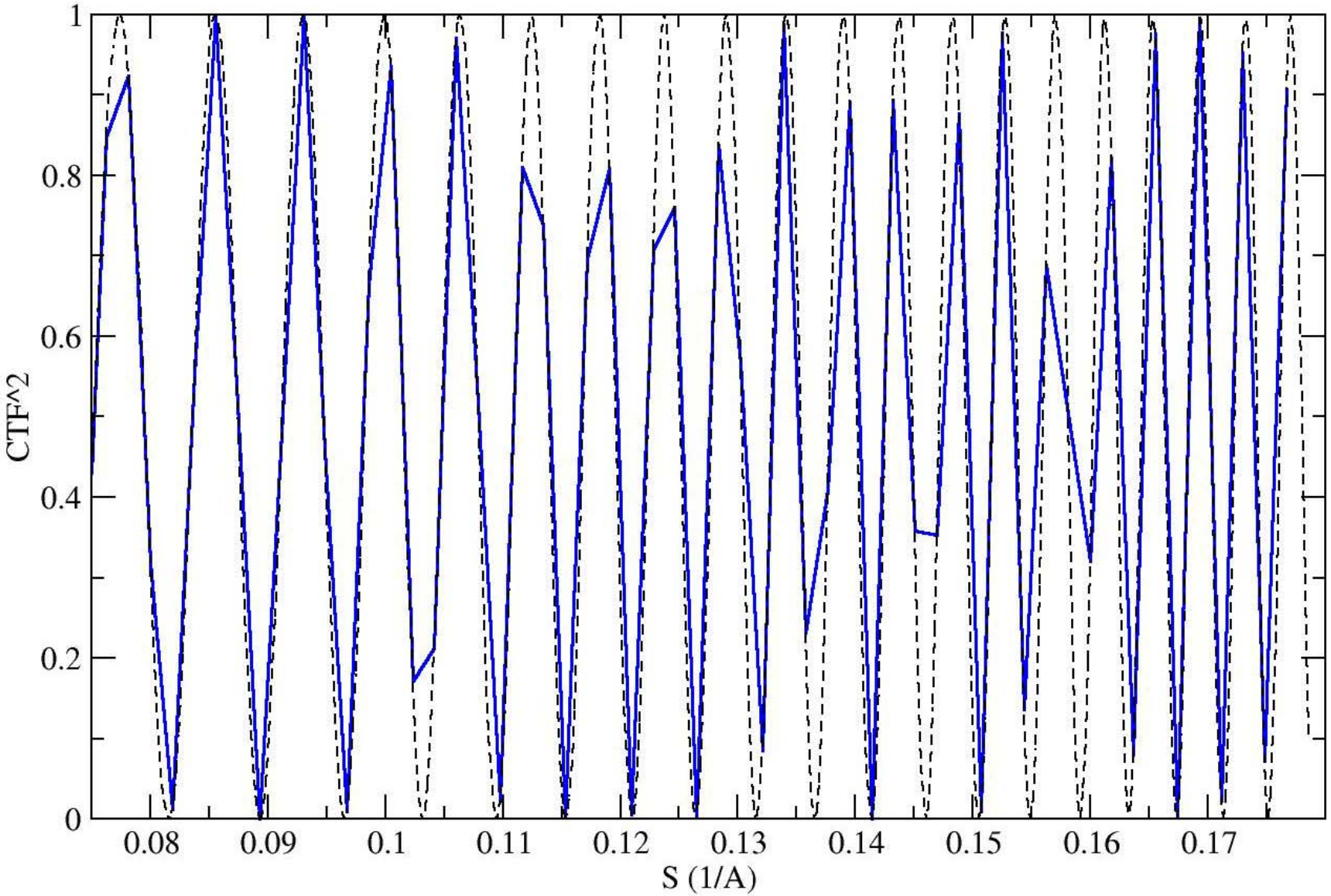

200 kV, Cs = 1.2mm, 2.8 A/pixel. 192x192 pixels box, ΔZ=3 µm

Effect of Particle Size on CTF Appearance

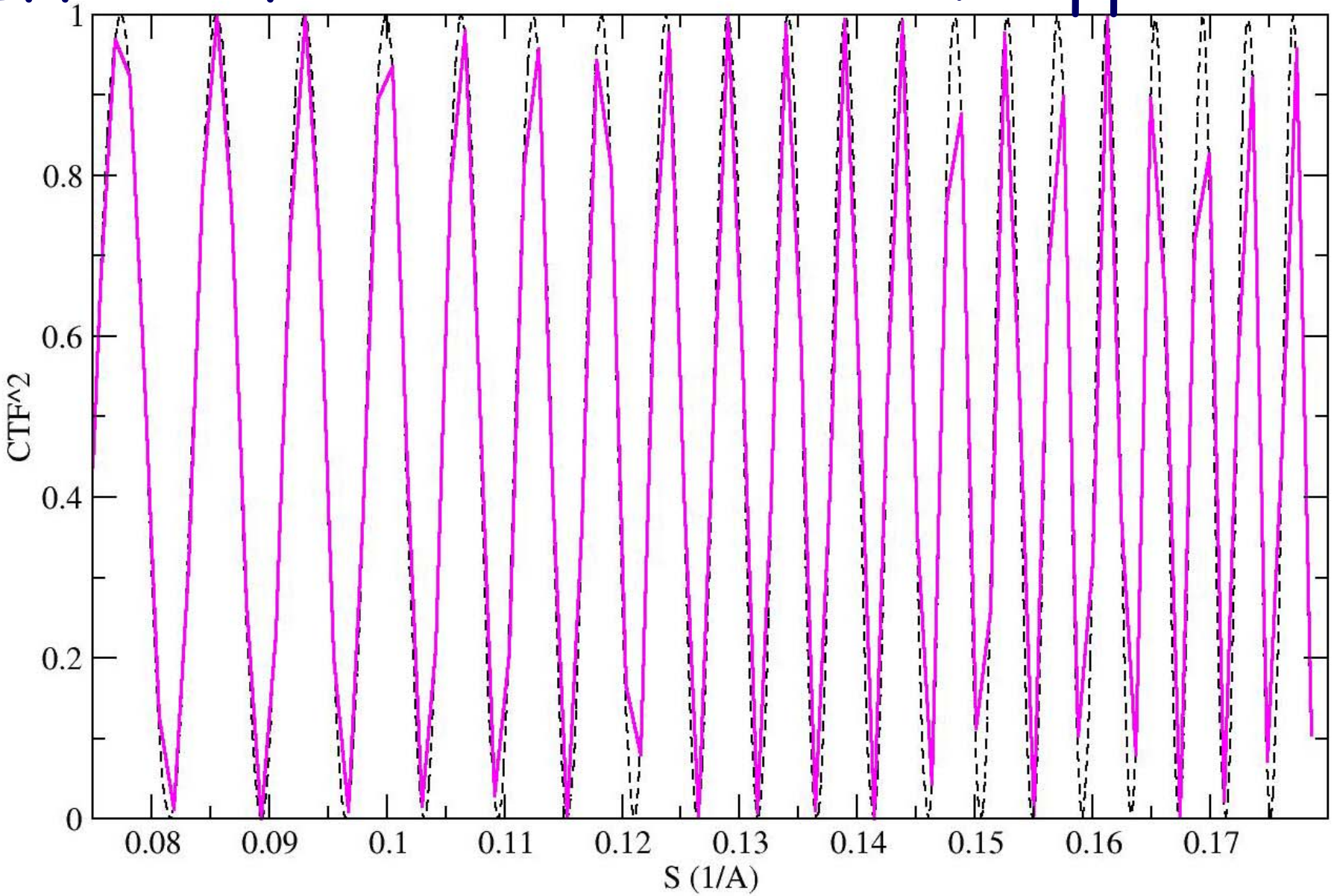

200 kV, Cs = 1.2mm, 2.8 A/pixel. 288x288 pixels box, ΔZ=3 μm

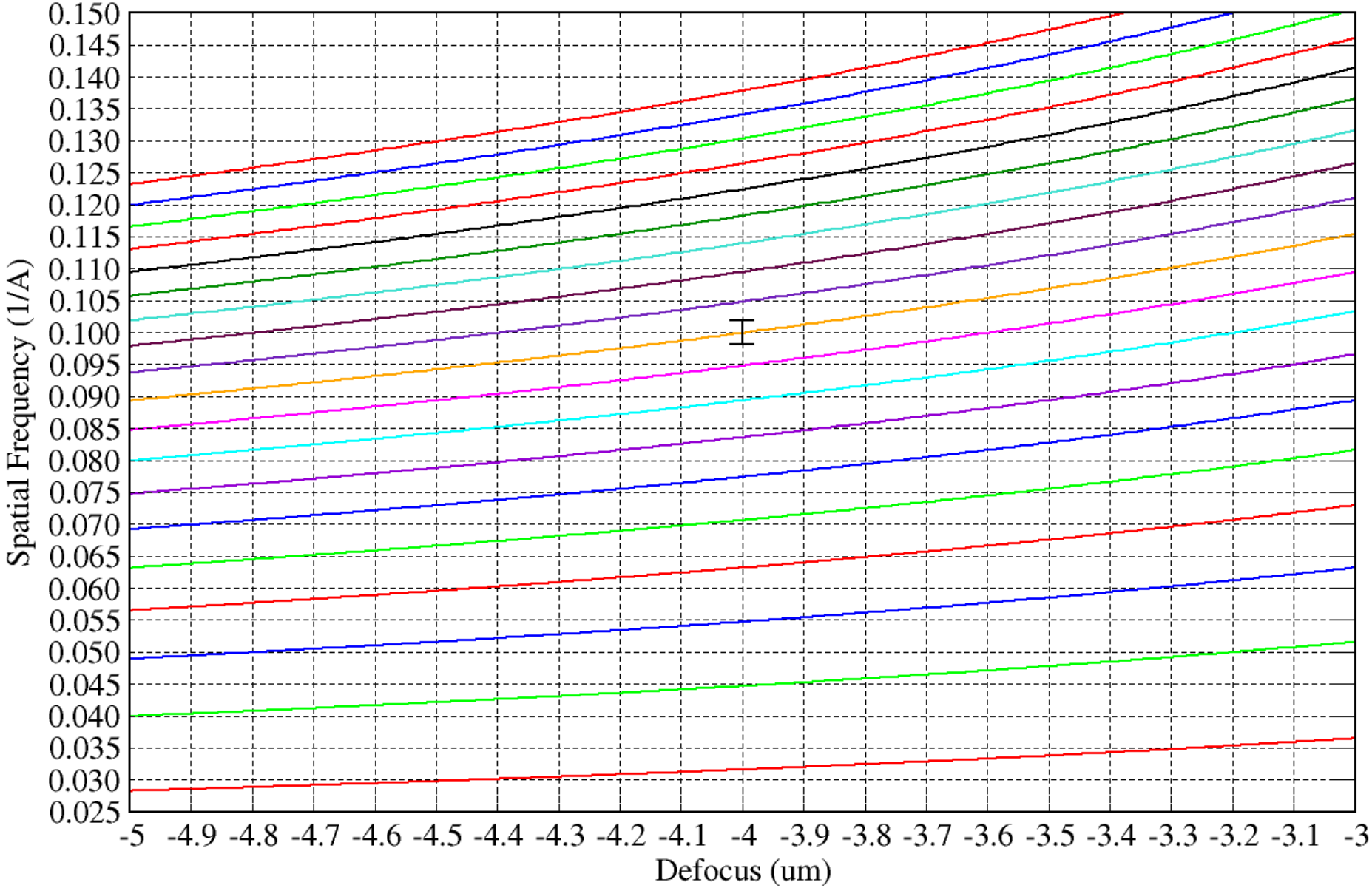
200kV, Cs 1.2mm
Spatial Frequency (1/A)
0.150
0.145
0.140
0.135
0.130
0.125
0.120
0.115
0.110
0.105
0.100
0.095
0.090
0.085
0.080
0.075
0.070
0.065
0.060
0.055
0.050
0.045
0.040
0.035
0.030
0.025
-5 -4.9 -4.8 -4.7 -4.6 -4.5 -4.4 -4.3 -4.2 -4.1 -4 -3.9 -3.8 -3.7 -3.6 -3.5 -3.4 -3.3 -3.2 -3.1 -3
Defocus (um)

CCD Camera for Single Particle Imaging

JEM2010F with a Gatan 4k CCD

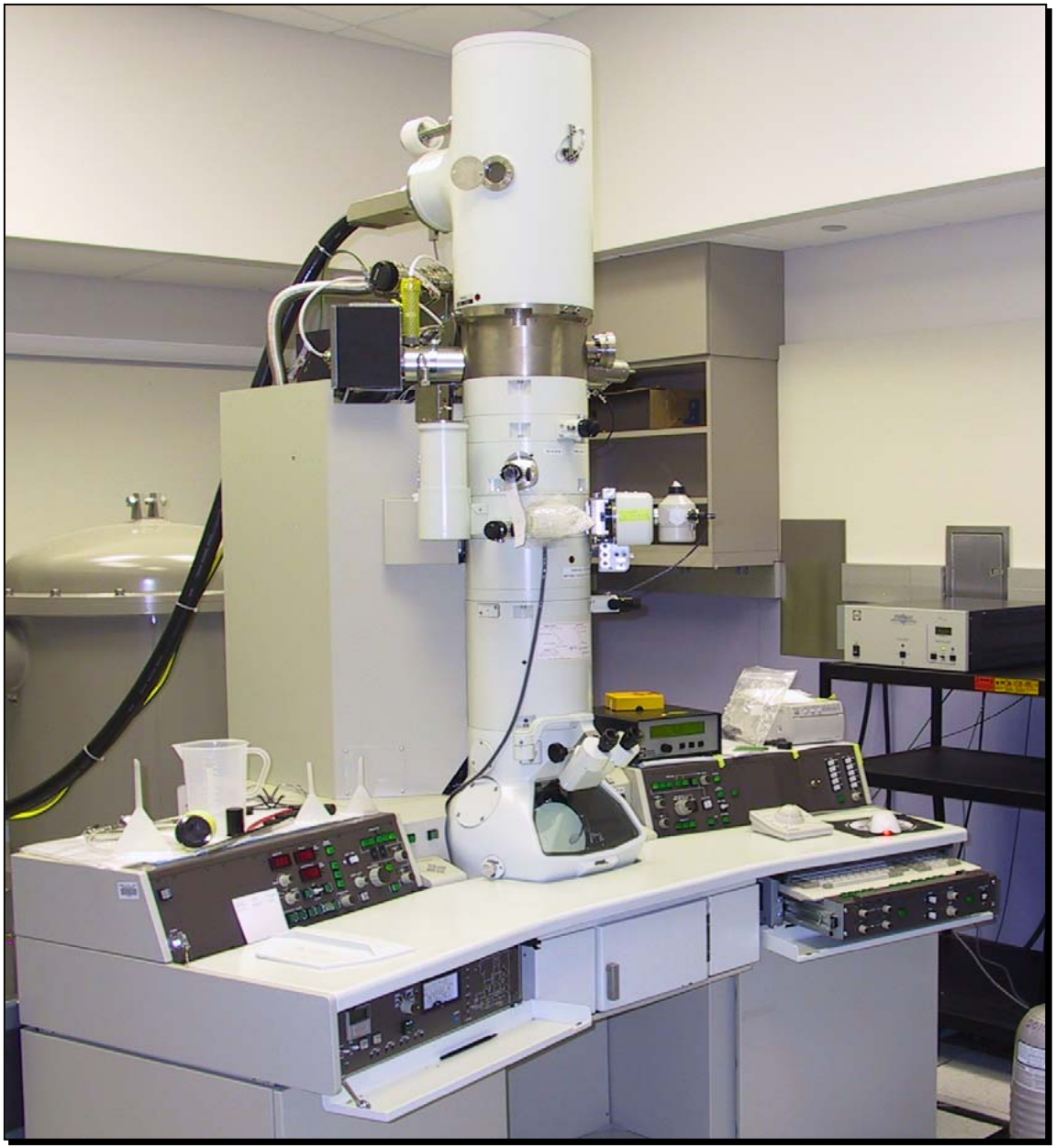

MTF of 4k CCD at 200 kV

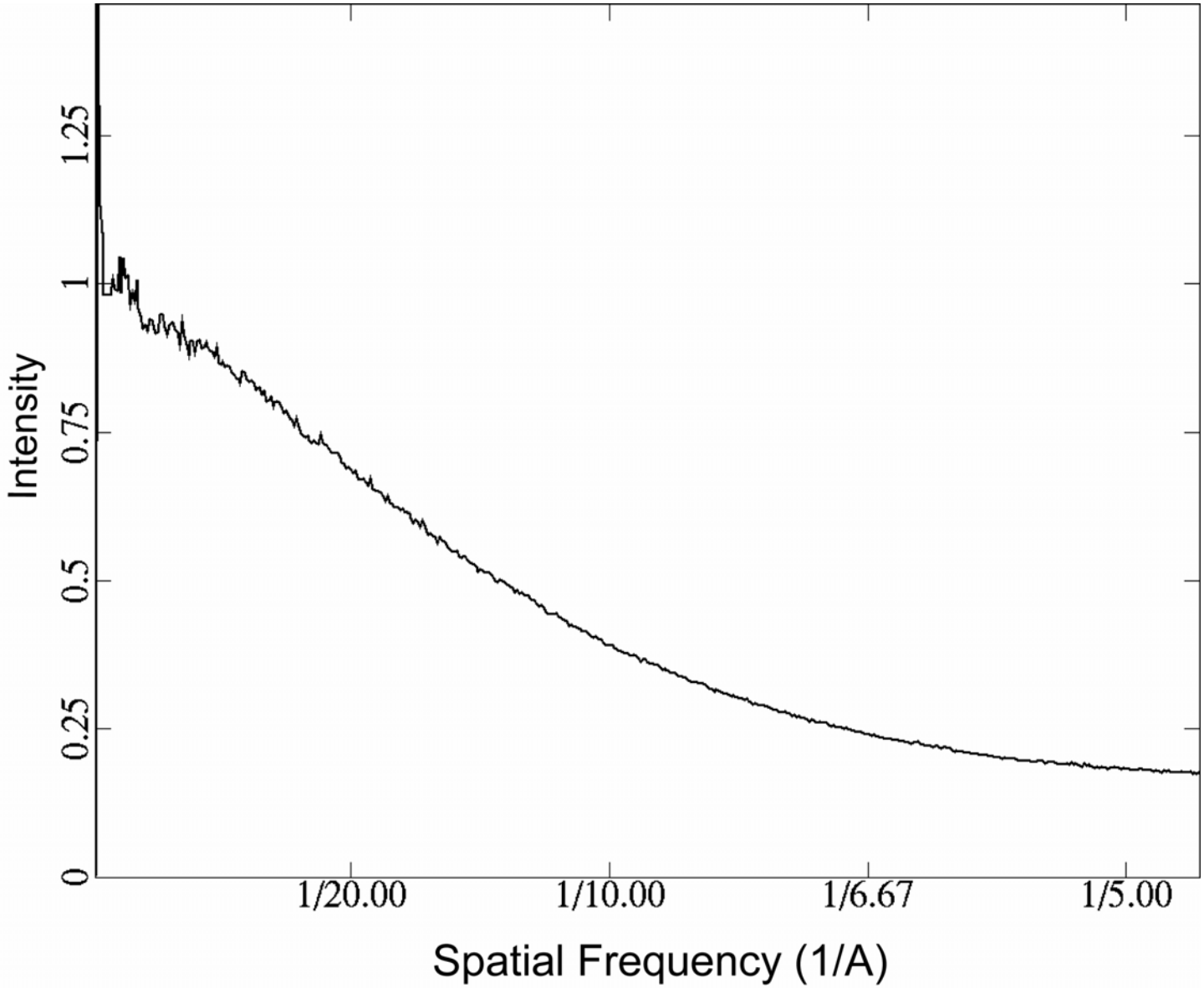

S/N of 200 kV Carbon Film Image

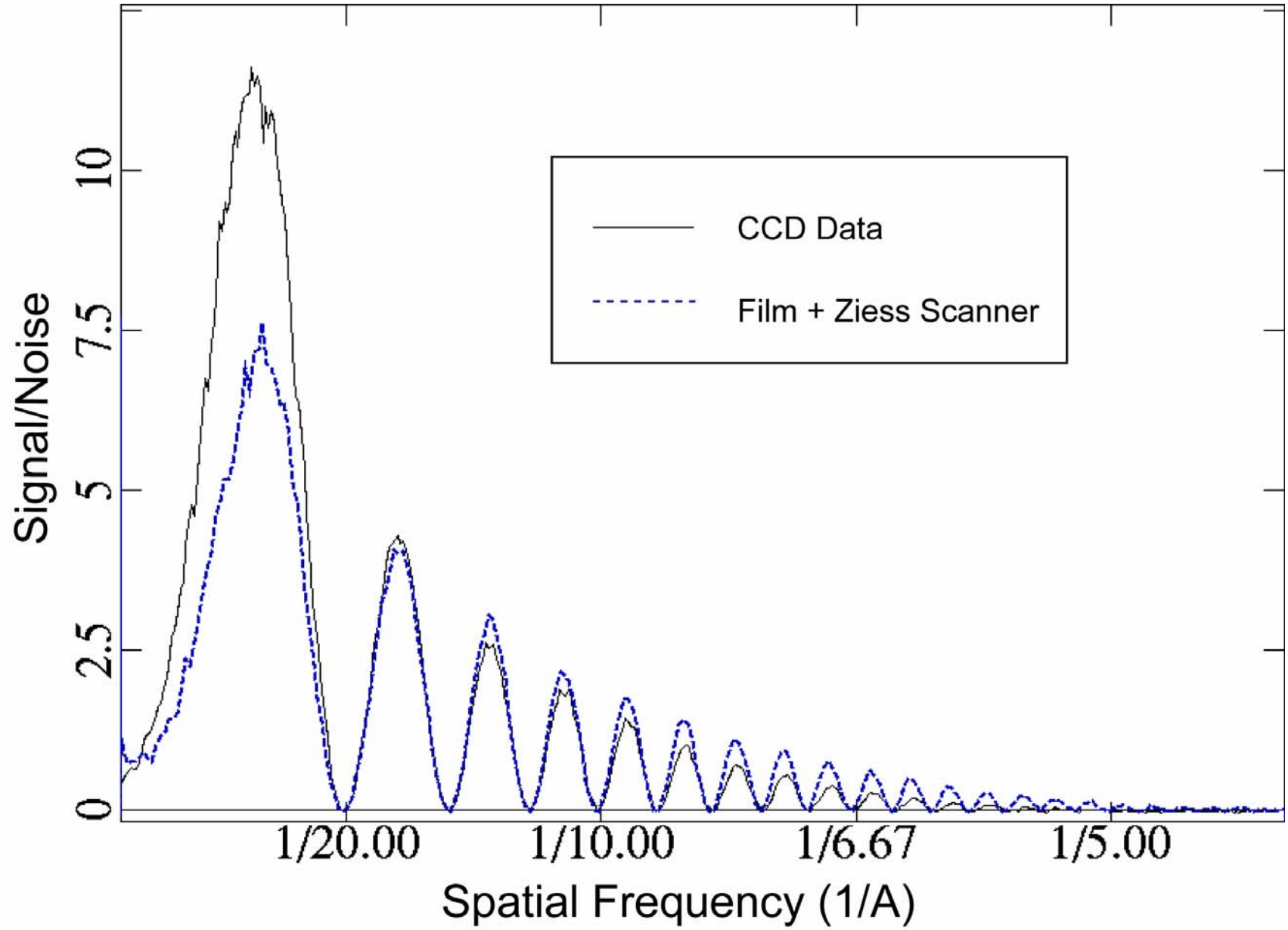

9Å Map of CPV from CCD Images

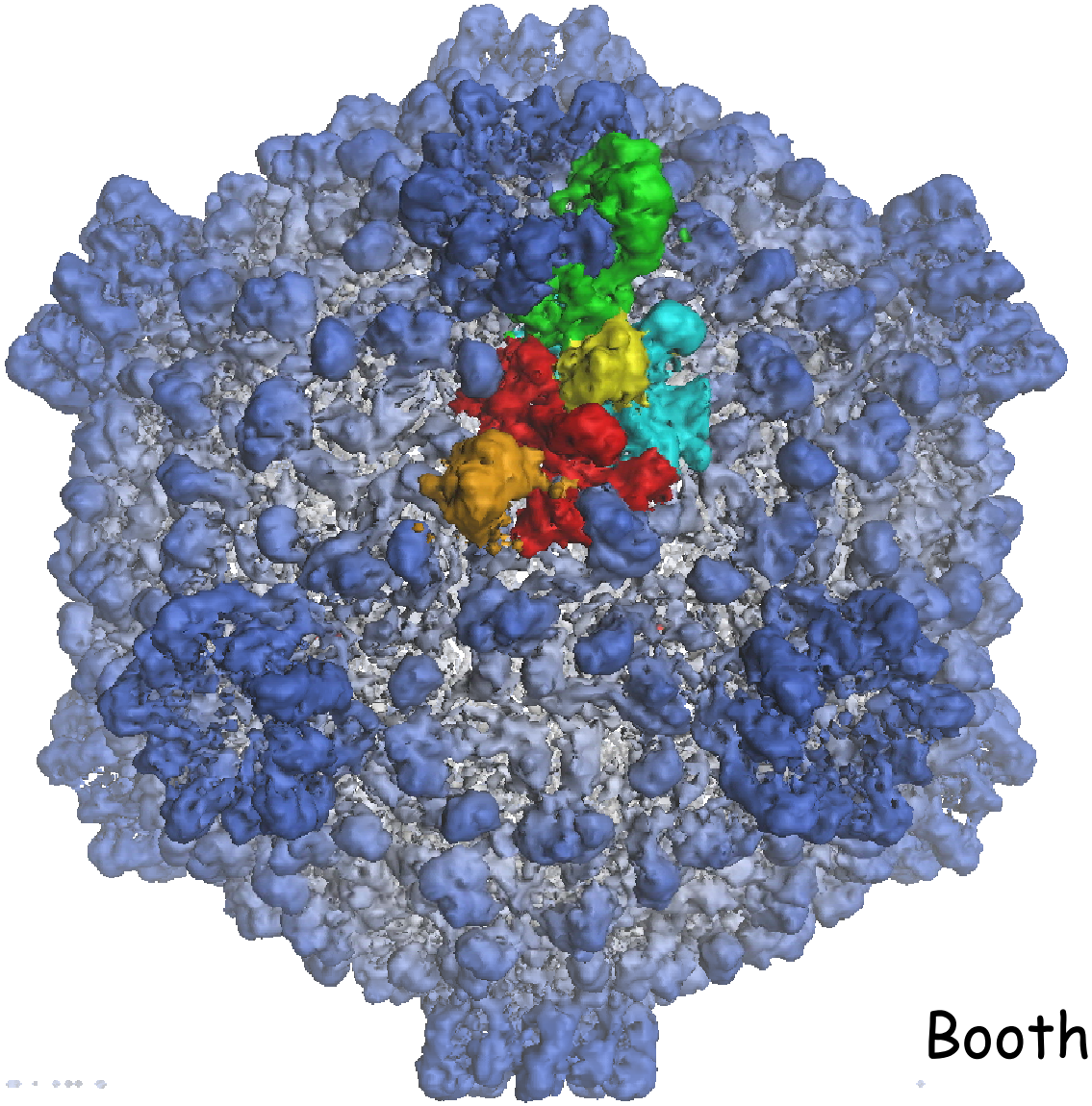

Booth et al, JSB 2004

Secondary Structure Elements in CSP-A

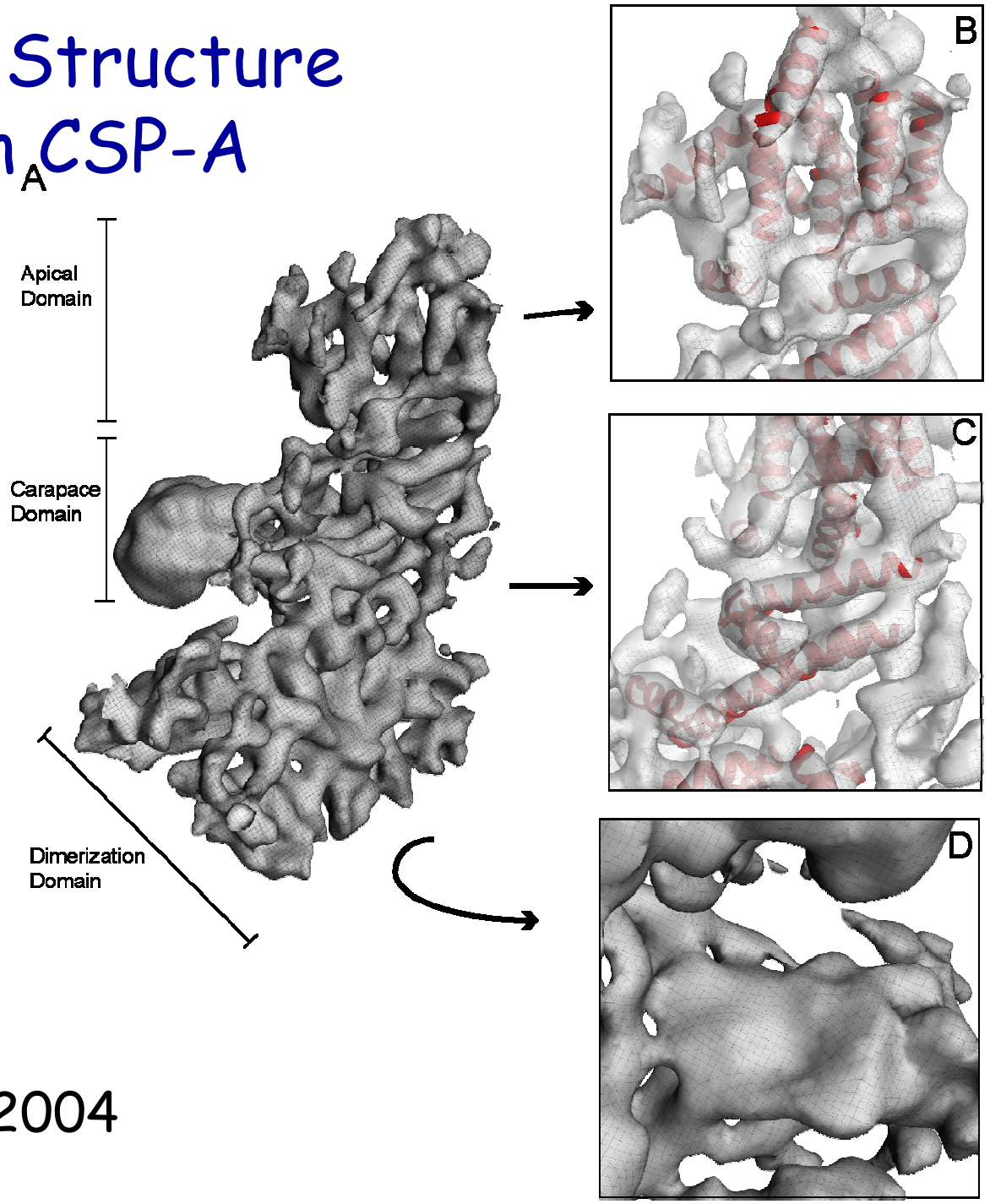

Booth, JSB, 2004

Magnification To Use For Higher Resolution Structure Study

Effective Microscope Magnification	Å/pix	Dimension of CCD Frame on Specimen (nm)	% CCD Frame Area wrt 82800 x	2/5 Nyquist (Å)
55,200	2.71	1,110	225	13.55
69,000	2.17	886	144	10.84
82,800	1.81	738	100	9.03
110,400	1.35	554	56	6.77
138,000	1.08	443	36	5.42
207,000	0.72	295	16	3.61

15 microns/pixel Gatan 4k CCD

References

Jiang, W. & Chiu, W. Web-based simulation for contrast transfer function and envelope functions. *Microsc & Microanal* **7**, 329-334 (2001).

Ludtke, S.J., Jakana, J., Song, J.-L., Chuang, D. & Chiu, W. A 11.5 Å single particle reconstruction of GroEL using EMAN. *J Mol Biol* **314**, 253-262 (2001).

Saad, A. et al. Fourier amplitude decay of electron cryomicroscopic images of single particles and effects on structure determination. *J Struct Biol* **133**, 32-42 (2001)

Zhou, Z.H. et al. CTF determination of images of ice-embedded single particles using a graphics interface. *J Struct Biol* **116**, 216-22 (1996).

Zhu, J., Penczek, P.A., Schroder, R. & Frank, J. Three-dimensional reconstruction with contrast transfer function correction from energy-filtered cryoelectron micrographs: procedure and application to the 70S E coli ribosome. *J Struct Biol* **118**, 197-219 (1997).

Toyoshima, C. & Unwin, P.N.T. Contrast transfer for frozen-hydrated specimens: Determination from pairs of images. *Ultramicroscopy* **25**, 279-292 (1988).

References

Chiu, W. Factors in high resolution biological structure analysis by conventional transmission electron microscopy. *Scanning Electron Micros* **1**, 569-580 (1978).

Wade, R.H. & Frank, J. Electron microscope transfer functions for partially coherent axial illumination and chromatic defocus spread. *Optik* **49**, 81-92 (1977).

Frank, J. Determination of source size and energy spread from electron micrographs using the method of Young's fringes. *Optik* **44**, 379-91 (1976).

Frank, J. The envelope of electron microscopic transfer functions for partially coherent illumination. *Optik* **38**, 519-36 (1973).

Thon, F. Phase contrast electron microscopy. in *Electron Microscopy in Material Sciences* (ed. Valdre, U.) 571-625 (Academic Press, Inc., New York, 1971).

Erickson, H.P. & Klug, A. The Fourier transform of an electron micrograph: effects of defocussing and aberrations, and implications for the use of underfocus contrast enhancement. *Phil. Trans. Roy. Soc. Lond. B* **261**, 105-18 (1970).

SIMULATION OF CTF

http://ncmi.bcm.tmc.edu/ncmi/software/software_details?selected_software=counter_30

5.10 Convolutions

$$c(\mathbf{u}) = \int_{\text{all } \mathbf{r}} f(\mathbf{r}) g(\mathbf{u} - \mathbf{r})\, d\mathbf{r} \tag{5.27}$$

This is known as the ***Convolution*** of $f(\mathbf{r})$ and $g(\mathbf{r})$, and may be written as $f(\mathbf{r}) * g(\mathbf{r})$.

$$c(\mathbf{u}) = f(\mathbf{r}) * g(\mathbf{r}) = \int_{\text{all } \mathbf{r}} f(\mathbf{r}) g(\mathbf{u} - \mathbf{r})\, d\mathbf{r}$$

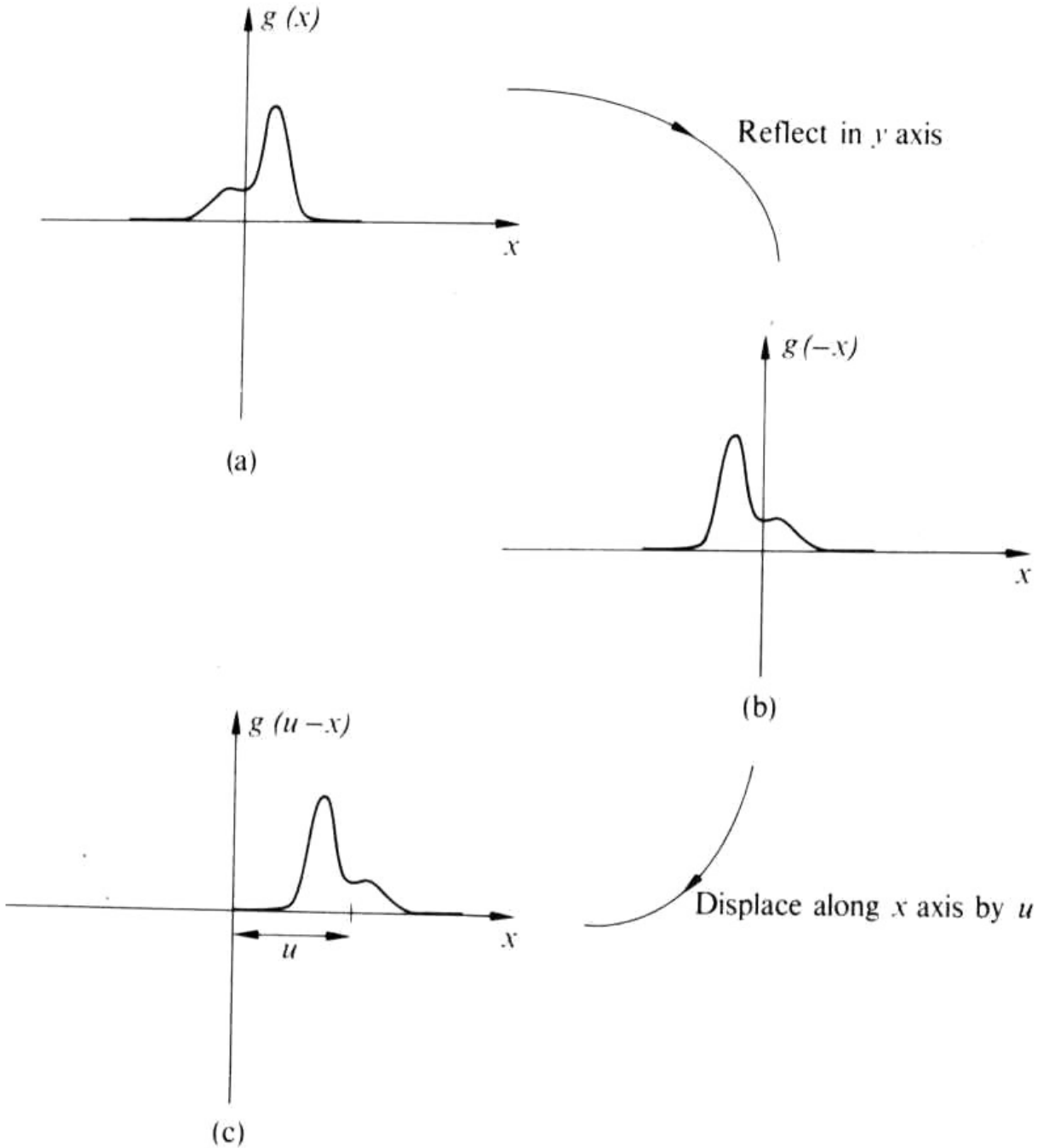
g (x)
x
(a)
Reflect in y axis
g (−x)
x
(b)
g (u − x)
u
x
(c)
Displace along x axis by u

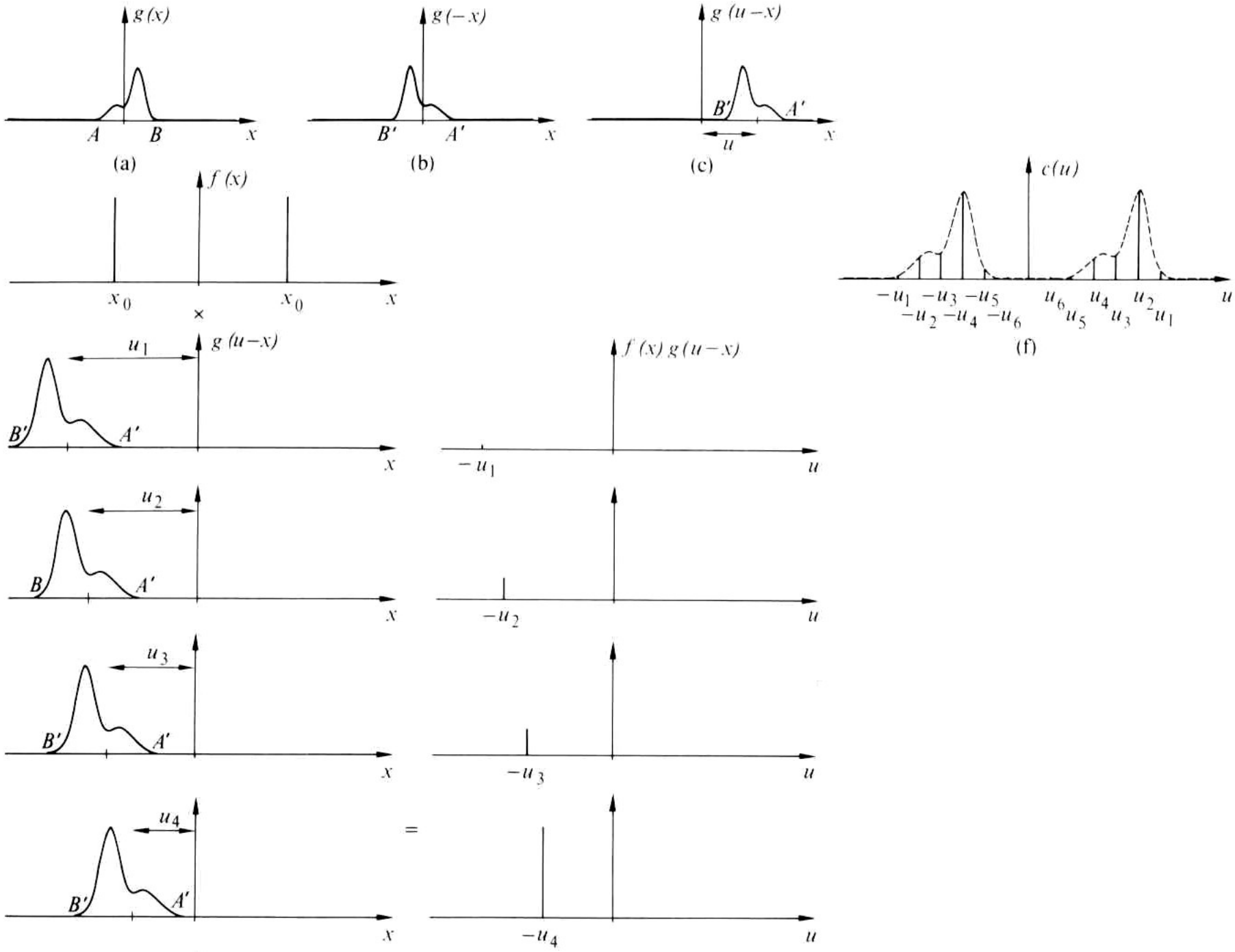
g (x)
A
B
x
(a)
g (−x)
B′
A′
x
(b)
g (u−x)
B′
A′
u
x
(c)
f (x)
x0
x0
x
×
u1
g (u−x)
B′
A′
x
f (x) g (u−x)
−u1
u
u2
B
A′
x
−u2
u
u3
B′
A′
x
−u3
u
u4
B′
A′
x
=
−u4
u
c(u)
−u1 −u3 −u5
−u2 −u4 −u6
u6 u4 u2
u5 u3 u1
u
(f)

$$l(\mathbf{r}) = \sum_{\text{all } p,\, q,\, r} \delta(\mathbf{r} - [p\mathbf{a} + q\mathbf{b} + r\mathbf{c}]) \qquad (5.17)$$

in which p, q and r correspond to allowed points defined by the lattice of unit vectors **a**, **b** and **c**. Our study of crystals in Chapter 3 told us that associated with each lattice point in a crystal is an identical unit cell. Suppose we represent the structure of the unit cell by some mathematical function of position $u(\mathbf{r})$, which we shall define as the ***Unit cell function***.

If we assume that the complete crystal may be represented by some mathematical function $c(\mathbf{u})$ which we shall call the ***Crystal structure function***, then we may write

crystal structure function = lattice function $*$ unit cell function

$$c(\mathbf{u}) = l(\mathbf{r}) * u(\mathbf{r})$$

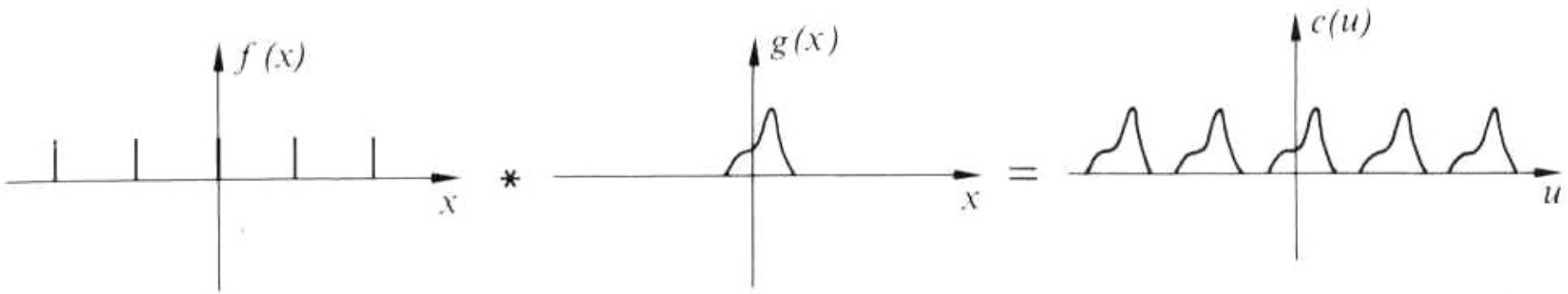

Fig. 5.19. *Convolutions with an array of* δ *functions.* If $f(x)$ is an array of δ functions, and $g(x)$ the arbitrary function shown, then the result of the convolution $f(x) * g(x)$ is to associate the g function with each δ function. This is always true on condition that $g(x)$ is narrower than the spacing of the δ functions so that $g(x)$ never overlaps two δ functions simultaneously.

$$Tc(\mathbf{u}) = T[l(\mathbf{r}) * u(\mathbf{r})]$$

$$= [Tl(\mathbf{r})] \cdot [Tu(\mathbf{r})]$$

FFT of a convolution function is equivalent to the product of FFTs of the two functions

3.3.8.2 Correlation

The correlation† of two continuous functions $f(x)$ and $g(x)$, denoted by $f(x) \circ g(x)$, is defined by the relation

$$f(x) \circ g(x) = \int_{-\infty}^{\infty} f(\alpha)\, g(x + \alpha)\, d\alpha \tag{3.3-36}$$

The forms of Eqs. (3.3-36) and (3.3-23) are similar, the only difference being that the function $g(x)$ is not folded about the origin. Thus, to perform correlation we simply slide $g(x)$ by $f(x)$ and integrate the product from $-\infty$ to ∞ for each value of displacement x. The procedure is illustrated in Fig. 3.18, which should be compared with Fig. 3.13.

---

†If $f(x)$ and $g(x)$ are the same function, Eq. (3.3-36) is usually called the *autocorrelation* function; if $f(x)$ and $g(x)$ are different, the term *crosscorrelation* is normally used.

5.12 The Patterson function

The final section of this chapter will deal with the properties of another integral which will be discussed in Chapter 11. A treatment of the mathematical behaviour of this integral is included here, since it is very similar to the convolution integral. Let us define the ***Patterson integral*** as

$$p(\mathbf{u}) = \int_{\text{all } \mathbf{r}} f(\mathbf{r})g(\mathbf{u}+\mathbf{r})\, d\mathbf{r} \tag{5.31}$$

Comparison of the Patterson integral with the convolution integral

$$c(\mathbf{u}) = \int_{\text{all } \mathbf{r}} f(\mathbf{r})g(\mathbf{u}-\mathbf{r})\, d\mathbf{r} \tag{5.27}$$

shows that the only difference between them is the fact that the Patterson integral has $g(\mathbf{u}+\mathbf{r})$ where the convolution integral has $g(\mathbf{u}-\mathbf{r})$. The general

Method for finding Patterson integrals $\int_{\text{all } \mathbf{r}} f(\mathbf{r})g\,(\mathbf{u}+\mathbf{r})d\mathbf{r}$

(1) $f(\mathbf{r})$ and $g(\mathbf{r})$ will be given functions.

(2) Displace $g(\mathbf{r})$ by any chosen $\mathbf{u}$ to form $g(\mathbf{u}+\mathbf{r})$.

(3) Each peak in the Patterson function $p(\mathbf{u})$ occurs at values of $\mathbf{u}$ corresponding to plus and minus the separation of any pair of peaks in the original function $f(\mathbf{r})$.

(4) The strength of each Patterson peak is the product of the strengths of the two peaks in the original function $f(\mathbf{r})$ which are separated by the corresponding value of $\mathbf{u}$.

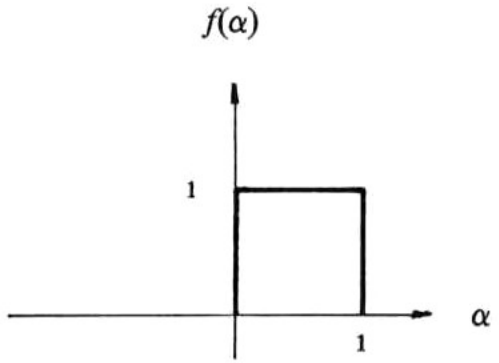
$f(\alpha)$
1
1
α

(a)

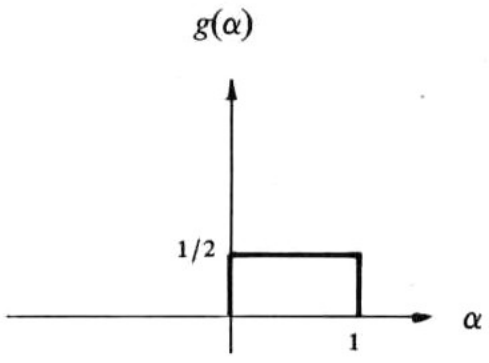
$g(\alpha)$
1/2
1
α

(b)

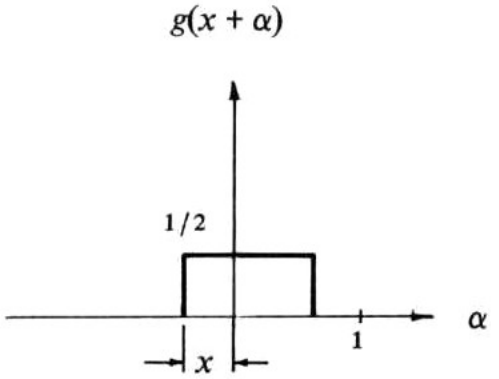
$g(x+\alpha)$
1/2
1
x
α

(c)

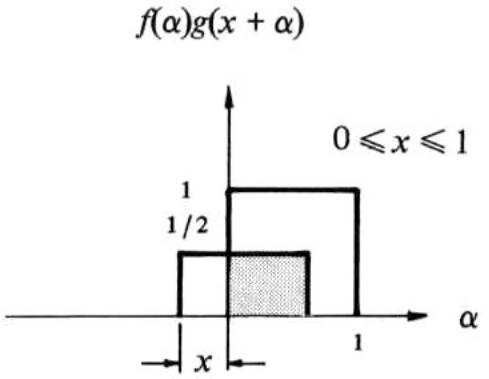
$f(\alpha)g(x+\alpha)$
$0 \leqslant x \leqslant 1$
1
1/2
1
x
α

(d)

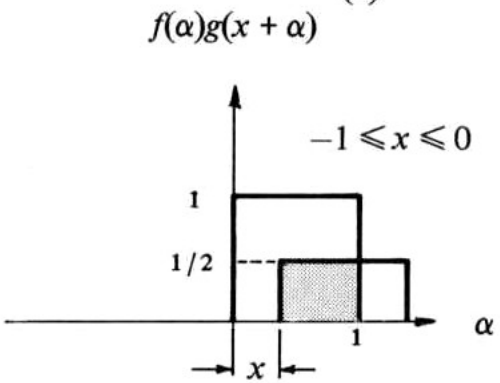
$f(\alpha)g(x+\alpha)$
$-1 \leqslant x \leqslant 0$
1
1/2
1
x
α

(e)

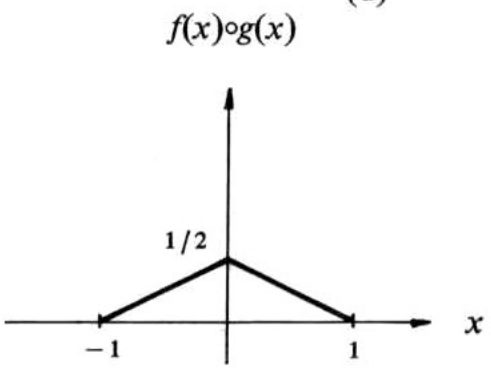
$f(x) \circ g(x)$
1/2
-1
1
x

(f)

Cross Correlation

$$C = F * G$$

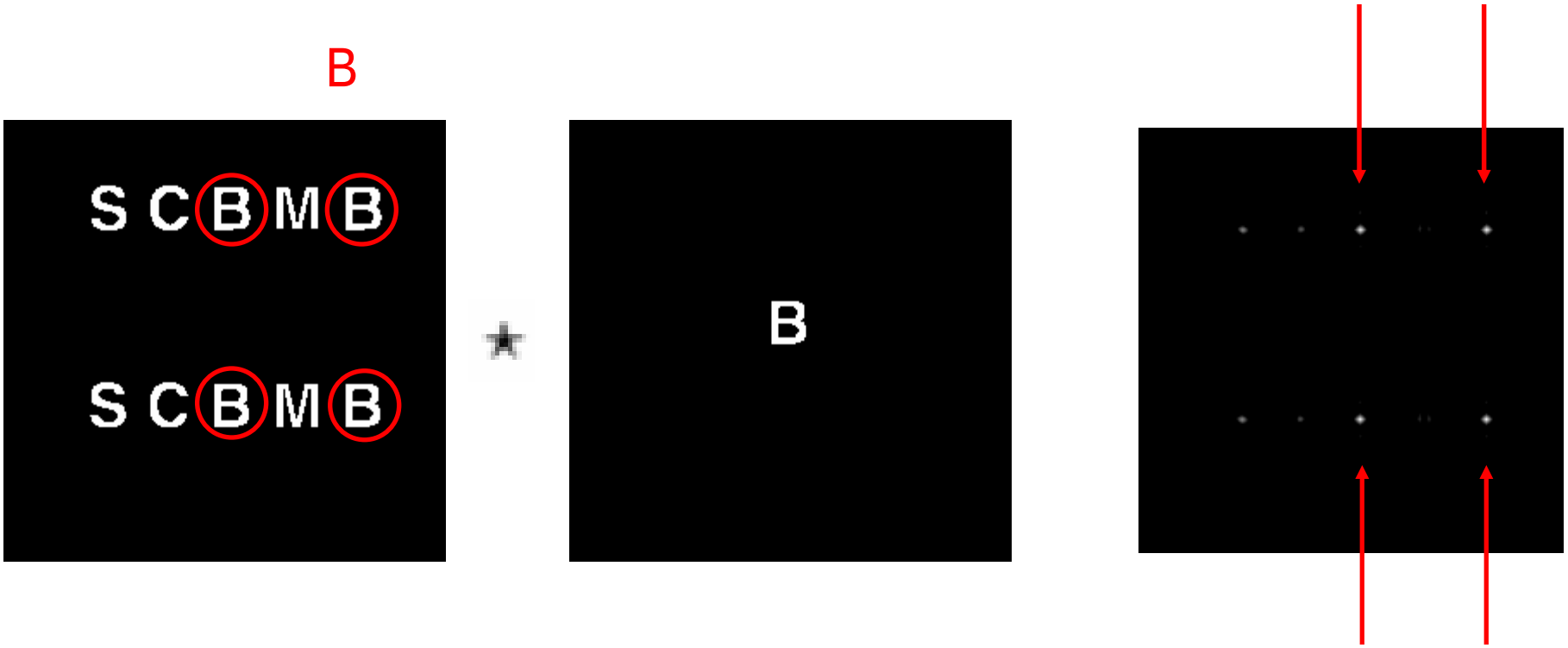

F G C